Environmental and Experimental Botany 209 (2023) 105287

Contents lists available at ScienceDirect

Environmental and Experimental Botany

journal homepage: www.elsevier.com/locate/envexpbot

Brassinosteroids interact with nitric oxide in the response of rice root systems to arsenic stress

D. Piacentini, F. Della Rovere, F. Lanni, M. Cittadini, M. Palombi, L. Fattorini, V. Cecchetti, M.M. Altamura, G. Falasca *

Department of Environmental Biology, Sapienza University of Rome, Italy

ARTICLE INFO

Keywords:
Arsenic
Brassinosteroids
Nitric oxide
Oryza sativa
OsNOS1 gene
Roots

ABSTRACT

Brassinosteroids (BRs), an emerging class of phytohormones, affect numerous plant physiological and metabolic processes and can improve plant defense systems to counteract metalloid phytotoxicity. Nitric oxide (NO), a reactive nitrogen species (RNS), behaves as a signalling molecule activating plant cellular responses to various environmental conditions. Brassinosteroids induce NO synthesis through nitrate reductase (NR) and NO synthase (NOS) activities. Arsenite and arsenate, inorganic forms of the metalloid arsenic (As), cause both soil pollution and many disorders in numerous plants, including important crops like rice, due to the oxidative stress generated by the imbalance between RNS and reactive oxygen species (ROS). Rice is very susceptible to As toxicity because both As availability and solubility are high in flooded paddy fields in many cultivated areas. The research aims to investigate the effects of BRs on the rice root systems exposed to 10^{-4} M $Na_2HAsO_4 0.7\ H_2O$ [$As^{(V)}$] or 2.5×10^{-5} M $NaAsO_2$ [$As^{(III)}$], highlighting the induced cyto-histological events and dissecting the NO role in the root response. A specific concentration (10^{-7} M) of 24-epibrassinolide (24-eBL), an exogenously applied BR, increases lateral root (LR) formation of more than 50% in the presence of $As^{(III)}$ or $As^{(V)}$. In addition, eBL attenuates the thickening of the cell walls induced by As in the outermost root cortical layers of LRs and in the adventitious roots (ARs) by reducing of ~ 50% the lignin deposition, while it restores the $As^{(v)}$-altered NO levels by increasing *OsNOS1* expression and the cellular NO distribution.

1. Introduction

Brassinosteroids (BRs) are a family of steroidal phytohormones involved in many physiological and metabolic processes in plants. They control cell division and elongation, seed germination, plant reproduction and senescence, and root system architecture including both the primary root (PR) development and the formation and development of lateral roots (LRs) and adventitious roots (ARs) (Yang et al., 2011). Furthermore, BR involvement in plant stress responses is recently gaining increasing interest across the plant research community (Nolan et al., 2020; Della Rovere et al., 2022). Brassinosteroids strengthen the plant defence system enhancing the tolerance to a plethora of both biotic (Sahni et al., 2016) and abiotic stresses (Wu et al., 2016; Della Rovere et al., 2022). The pathways involved in this response include the antioxidant system activation, the modulation of gene expression, and the crosstalk with other phytohormones, resulting in a finely tuned signal cascade able to regulate plant growth in non-optimal conditions (Anwar et al., 2018; Vardhini, 2017).

As with other phytohormones, also BRs effect on root development depends on their levels. In fact, low concentrations of BRs generally promote root growth, while high concentrations inhibit it, as highlighted in *Arabidopsis thaliana* (L.) Heynh. (Arabidopsis) and *Oryza sativa* (L.) (rice) (Chaiwanon and Wang, 2015; Jantapo et al., 2021; Della Rovere et al., 2022). In Arabidopsis root apical meristem, BRs interact with auxin establishing a concentration gradient mainly in the stem cell niche (Dolan et al., 1993; Pardal and Heidstra, 2021). This is necessary to regulate the spatio-temporal balance between the stem cells, which divide infrequently, and the surrounding cells destined, instead, to differentiate (Chaiwanon and Wang, 2015). Moreover, nanomolar concentrations of BRs promote the early exit of cells, destined to differentiate, from the apical meristem, thus affecting both the overall size of the meristem (Fridman et al., 2021, and references therein) and the rate of cell expansion/distension extent in the root elongation zone, responsible for the organ growth (Beemster and Baskin, 1998). Indeed, in

* Corresponding author.
E-mail address: giuseppina.falasca@uniroma1.it (G. Falasca).

https://doi.org/10.1016/j.envexpbot.2023.105287
Received 7 December 2022; Received in revised form 10 February 2023; Accepted 2 March 2023
Available online 4 March 2023

Arabidopsis BRs are known to interact with auxin in a dual way, by simultaneously promoting auxin biosynthesis and repressing auxin signalling output. This dual mechanism is required for maintaining the correct functionality of the entire root meristem (Ackerman-Lavert et al., 2021). In the same plant, Della Rovere and co-workers (2022) have demonstrated that, even in the presence of a strong environmental pollutant, such as cadmium (Cd), relatively low levels of exogenous BRs (24-epibrassinolide, eBL) are able to counteract the disruption of the quiescent centre (QC) induced by Cd. The QC, located in the centre of the stem cell niche, is responsible for the regular stem cells activity and it is induced and maintained in its state by auxin (Dolan et al., 1993; Della Rovere et al., 2013). The deleterious effects of Cd on the QC results in an auxin delocalization both in the PR, LR and AR apical meristems (Fattorini et al., 2017; Ronzan et al., 2018).

Exogenous treatments with biologically active forms of BRs, such as 24-epicastasterone, and with inhibitors of their biosynthesis (e.g., propiconazole), have shown that, similarly to auxin, also BRs affect root meristem size and cells elongation in a dose-dependent manner (Zhang et al., 2022).

Interactions between BRs and small molecules, such as reactive oxygen (ROS) and nitrogen (RNS) species, in plant physiological and stress responses are recently being demonstrated (Hu et al., 2021). The function of these reactive molecules in plant growth is particularly interesting due to their dual role, as stressors or signalling molecules, depending on their levels and reciprocal cellular balance (Piacentini et al., 2020a). Indeed, ROS and RNS activate many physiological and metabolic processes but might also be dangerous by triggering substantial damage to the cellular structures. Exogenous BR application enhances the activity of antioxidant enzymes that, in turn, reduce the stress provoked by ROS by activating their scavengers, as seen in maize, mustard, radish, wheat and rice plants exposed to metal stress (Rajewska et al., 2016 and references therein).

Nitric oxide (NO) is a multifunctional cell signalling RNS able to interact with ROS (Mansoor et al., 2022) and to exhibit a key role in numerous plant development processes and responses to environmental stresses (Corpas et al., 2009), including those caused by toxic metals (Piacentini et al., 2020a; b).

In plants, NO synthesis occurs mainly via the nitrate/nitrite reductase pathway catalysed by nitrate reductase (Gupta et al., 2011) and by the NO synthase (NOS)-like enzyme(s) through the L-arginine-dependent pathway (Simontacchi et al., 2015). In detail, the NOS-like enzyme (s) oxidize(s) arginine to citrulline and generate(s) the intermediate NO (Correa-Aragunde et al., 2013). NOS enzymes were originally identified and characterized in mammalian tissues, with various isoforms being localized in different cell types (Stuehr, 1999). In 2010, a *NOS* gene was identified for the first time in a photosynthetic organism, namely the green alga *Ostreococcus tauri* (Foresi et al., 2010). Although in plants the *NOS* genes have not been well characterized yet (Hurali et al., 2022), a putative Arabidopsis *NOS* gene (*AtNOS1*), encoding a protein sharing the amino acid sequence with a protein involved in NO synthesis in the snail *Helix pomatia,* was reported. In the same study, a loss of function mutant of *AtNOS1* showed impaired NO production and about a 25% reduction of NOS activity (Guo et al., 2003).

Recently, a NOS activity has also been reported in rice roots and has been shown to increase rapidly under drought stress (Cao et al., 2019). However, we are still very far from understanding the role of NOS enzyme(s) in the synthesis of NO in plants, as well as in identifying their tissue localization, especially when plants are exposed to adverse environmental conditions.

It has been demonstrated that NO can reduce the cellular oxidative stress caused by heavy metal exposition (Emamverdian et al., 2021 and references therein). In Arabidopsis and rice exposed to Cd and arsenic (As), NO modulates/restores root system architecture (Praveen and Gupta, 2018; Piacentini et al., 2020a; b) and in maize increases As tolerance (Kaya et al., 2020). Likewise, NO can trigger the formation and development of ARs and can affect the root biomass in rice exposed to arsenate [$As^{(V)}$] by maintaining the ascorbate redox state and the cell cycle dynamics within optimal limits (Kushwaha et al., 2019). Moreover, it is known that BRs induce NO synthesis through nitrate reductase (NR) and NO synthase (NOS) pathways, probably to positively modulate plant growth under stressful conditions (Hu et al., 2021, and references therein).

Arsenic pollution is a huge environmental problem that causes concern both for agricultural soil contamination, as the metalloid enters the food chain, and for its effects on the biotic component of ecosystems. Depending on its redox state, As is found in soils mainly as inorganic $As^{(V)}$ or arsenite [$As^{(III)}$]. These forms affect plant development, animal health, and the general balance of ecosystems. In plants exposed to As, several toxicity symptoms have been reported, ranging from the reduction of root and shoot biomass, nutrient uptake, fruit, and grain yields, to reduction in seed germination, leaf necrosis, loss of chlorophyll content and photosynthesis ability (Ronzan et al., 2018; Piacentini et al., 2020b; Farooq et al., 2022 and references therein). Arsenate is taken up by the roots through phosphate transporters and, once inside the root, it can alter phosphate metabolism. In the root, $As^{(V)}$ is mainly reduced to $As^{(III)}$ but it is also possible that $As^{(III)}$ is re-oxidated to $As^{(V)}$ within the cell (Zvobgo, 2022).

Plants absorb $As^{(III)}$ via various proteins, such as the bidirectional Nodulin 26-like Intrinsic Protein (NIP) transporters which allow $As^{(III)}$ to move in both directions between plant cells, and the silicon (Si) transporters (LSi) due to the similarities between $As^{(III)}$ and Si (Abbas et al., 2018, and references therein). In rice, the LSi1 and LSi2 transporters have been reported to be located at the proximal and distal sides of the root exodermal and endodermal cells, facilitating the transport of $As^{(III)}$ across root cells and tissues (Ma et al., 2008). The damages that the inorganic As species cause in the roots are well documented, with $As^{(III)}$ being more toxic than $As^{(V)}$ when applied at the same concentration, as shown in rice (Piacentini et al., 2020a). At the cellular level, the roots exposed to As show an increase in cell width, cell wall lignification, widespread plasmolysis, and alteration of the cytoskeletal structures leading to a change in all tissues, as well as, an increase in diameter and modification of root length (Lou et al., 2015; Ronzan et al., 2018).

Rice is a crop that feeds most of the world's population and is widely cultivated throughout the world (Samal et al., 2021). However, rice consumption can cause As toxicity in humans due to the ease with which rice absorbs the metalloid from the soil. Unfortunately, a wide part of rice paddy fields in the world present high concentrations of As, especially in countries where the rice consumption *per capita* is higher. As the metalloid availability and solubility are very high under normal conditions of flooding, rice is very susceptible to As toxicity and prone to accumulate it in plant organs and grains (Wang et al., 2015). It is, therefore, important to identify strategies that can be used both to stimulate plant natural defences against As toxicity and to limit its accumulation in edible grains. In recent years the biosynthetic, degradation, and signalling pathways of BRs have been elucidated, as well as their multiple roles in plant growth and stress responses, e.g. in alleviating Cd stress in *Pisum sativum* seedlings (Jan et al., 2018). Nevertheless, the molecular functions and cyto-histological effects of BRs in response to As still need to be investigated. In fact, unlike heavy metals, where the ameliorative effects of BRs are known, evidence on the effects of these phytohormones in As-stressed plants is limited (Betti et al., 2021). In *Brassica juncea,* BRs, like 24-eBL, are synthetized after $As^{(V)}$ treatments, pointing out an involvement of BRs in conferring As-induced stress protection at least in this plant (Kanvar et al., 2015). In radish seedlings growing under toxic levels of As, 24-eBL and 28-homobrassinolide applications increase the activity of various antioxidant enzymes, further supporting the protective role of BRs against As toxicity (Raghu et al., 2014; Vardhini and Anjum, 2015).

Considering the limited studies on few plant species performed, in this work we investigated the effects of BRs on the architecture of rice root systems when exposed to $As^{(V)}$ or $As^{(III)}$ toxicity. The mechanisms activated at the cyto-histological level and the NO role in the root system

responses were also investigated. The results showed that exogenous eBL, when applied at a specific concentration, has multiple effects: i) increases LR formation in the presence of $As^{(III)}$/$As^{(V)}$; ii) attenuates the lignin thickening of the cell walls induced by As in the outermost cortical layers of LRs and ARs; iii) restores the $As^{(V)}$-altered NO levels by increasing *OsNOS1* expression and cellular NO distribution. The possibility that the positive effects of BRs in alleviating the damages caused by As also involve the NO as a modulator is discussed.

2. Methods

2.1. Plant material and growth conditions

Seeds of *Oryza sativa* ssp. Japonica (cv. Nihonmasari) were surface sterilized according to Ronzan and co-workers (2018), and then sown in sterile poly-ethylene terephthalate (PETG) vessels with a rectangular base (11.4 × 8.6 × 10.2 cm) (Phytatray™ II, Sigma-Aldrich, Saint Louis, MO, USA), each containing 100 mL of half-strength (2.1 g L^{-1}) Murashige and Skoog (Murashige and Skoog, 1962) medium, 0.1% sucrose and 0.8% agar at pH 5.6–5.8 (Control medium). Arsenic treatments were performed by adding 2.5 × 10^{-5} M $NaAsO_2$ [$As^{(III)}$] or 1 × 10^{-4} M $Na_2HAsO_4{\cdot}7\ H_2O$ [$As^{(V)}$] to the Control medium. The concentrations of the two As salts were chosen based on our previously published results (Piacentini et al., 2020a). The 10^{-6} M or 10^{-7} M or 10^{-8} M 24-epibrassinolide (eBL, Sigma-Aldrich-E1641, Saint Louis, MO, USA) concentrations were prepared starting from a 10^{-4} M eBL stock solution and were, then, added to the Control medium. These 24-eBL concentrations were chosen in accordance with our previous work and the literature data (Guedes et al., 2021; Della Rovere et al., 2022). The eBL 10^{-4} M stock solution was obtained by dissolving the hormone in 10% ethanol (EtOH). This low EtOH concentration was previously tested for no negative effects on seed germination and root growth (Della Rovere et al., 2022). Finally, the combined treatments were prepared by adding to the culture medium the different eBL concentrations with $As^{(III)}$ or $As^{(V)}$ salts at the concentrations above mentioned. All the eBL concentrations used in this study were administered to the media after the autoclave sterilization cycle and when the temperature was low enough (50–55 °C) to allow hormone stability. Thirty seeds, distributed in 6 Phytatrays (5 seeds per each phytatray), were sown for each condition and kept in a growth chamber in long-day regime (14 h light/10 h dark) for 10 days at 210 μmol $m^{-2}s^{-1}$ intensity of white light and under controlled temperature (27–28 °C light/25–26 °C dark). The relative humidity inside the vessel was about 98–99%. All the experiments were performed in three independent biological replicates with similar results.

2.2. Morphological analyses

To evaluate the possible mitigatory effects of eBL on rice root systems exposed to As, a morphological analysis was performed on roots of seedlings grown for 10 days in the presence of the eBL treatments (10^{-6} M, 10^{-7} M or 10^{-8} M), combined or not with $As^{(III)}$ or $As^{(V)}$ salts. The adventitious root (AR) length, the lateral root (LR) density, and the fresh root-system biomass were evaluated from thirty seedlings per treatment at day 10, when the primary root (PR) had already stopped growing. The AR length was measured under a LEICA MZ8 stereomicroscope (Leica Microsystems, Germany) using Zeiss Zen 2.3 software from digital images captured with Zeiss AxioCam camera (Zeiss, Germany) and expressed as mean length (cm) ± S.E. The LR density was obtained by acquiring images of entire ARs with a Leica DMRB optical microscope (Leica Microsystems, Germany) equipped with an OPTIKA C-P20CC camera (Optika, Italy) and counting all lateral root primordia (LRPs) and elongated LRs per each AR. The corresponding mean density was obtained as the ratio of the total LRs/LRPs number per cm of AR (± S.E.). Some ARs per treatment were cleared with chloral hydrate solution (Weigel and Glazebrook, 2002), mounted on microscope slides and observed with Nomarski optics applied to a Leica DMRB microscope.

Finally, the fresh root biomass was obtained by separating the roots from the aerial organs of the seedling and weighing them by a high sensitivity analytical balance (Kern ABT 220–5DNM; Kern & Sohn, Balingen, Germany), and weights were expressed as mean values [(g) ± S.E.].

Based on the morphological results (see Results), the eBL concentration of 10^{-7} M was chosen for the subsequent analyses.

2.3. Histological and lignin autofluorescence analyses

At day 10, the apical regions (about 2.0 cm from the root tip) of five ARs, exposed or not to eBL 10^{-7} M, $As^{(III)}$, or $As^{(V)}$, alone or combined, were fixed in 70% (v/v) ethanol, dehydrated with an ethanol series, embedded in Technovit 7100 (Heraeus Kulzer, Germany), longitudinally and transversally sectioned at 8 μm with a Microm HM 350 SV microtome, stained with 0.05% toluidine blue, and observed under a light microscope (Leica DMRB). To detect the extension of lignin deposition in the cell walls of the sclerenchyma and the outermost cortical layers, the lignin autofluorescence was observed under UV light in transverse, not-stained, sections taken up from the primary structure region of the ARs. Fluorescence quantification was performed on each AR section by a multi-point detection of the signal intensity in the target tissues and by assigning to each pixel a value ranging from 0 (pure black) to 255 (pure white) of arbitrary units (A.U.) by ImageJ software (version 1.53c, Wayne Rasband, National Institutes of Health, Bethesda, USA. Available online: https://imagej.nih.gov/ij, accessed on 09/2021).

2.4. Detection and quantification of nitric oxide in rice root system

At day 10, 5 ARs with forming LRs were taken from the root system of seedlings exposed or not to eBL 10^{-7} M, $As^{(III)}$, or $As^{(V)}$, alone or combined with eBL, and treated for NO visualization according to Piacentini et al. (2020a). Briefly, the ARs were incubated in darkness with 1 × 10^{-4} M of the specific NO-fluorescence probe 4-amino-5-methylamino-2′, 7′-difluorofluorescein diacetate (DAF-FM DA, Sigma-Aldrich, Saint) in 0.02 M HEPES/NaOH (pH 7.4) buffer for 30 min and at 25 °C. After incubation, the roots were washed three times with the buffer alone to remove probe excess and immediately observed under an Axio Imager M2 microscope (Zeiss, Oberkochen, Germany) motorized on the 3 axes using filters with BP455–495 nm excitation and BP505–555 nm emission wavelengths. Both single-plane and merged Z-stack images were acquired, and the quantification of the fluorescence signal was performed in the ARs and LRs apices including the root cap, the root meristem, and the elongation and differentiated zones. The fluorescence intensity in the region of interest was performed following the same methodology as for lignin detection and expressed in grayscale (from 0 to 255 of A.U.) by using Zen 2.5 (Zeiss) image analysis software. The analysis of NO in the lateral root primordia (LRPs) was performed only qualitatively to avoid errors in the signal quantification due to the interference with the fluorescent signal arising from the overlying AR tissues.

2.5. In situ hybridization of a putative OsNOS1 gene in rice roots

The choice of using *OsNOS1* (gene ID: 4328006) as a putative rice NO synthase gene arises from the high rate of similarity (74.27%) found between the OsNOS1 and the AtNOS1 aminoacidic sequences through FATCAT algorithm (Ye and Godzik, 2004) as reported in Supplementary Figure 1.

Total RNA was extracted from the roots of the Control seedlings using the “Spectrum - Plant Total RNA Kit” (Sigma-Aldrich, Saint Louis, USA) according to the manufacturer’s instructions and quantified using a NanoDrop™ One Spectrophotometer (Thermo Fisher Scientific, Inc.). For cDNA synthesis, 1 μg of total RNA was reversely transcribed using SensiFAST™ Reverse Transcriptase cDNA Synthesis Kit (Bioline,

London, UK) according to the manufacturer's instructions. Reverse-transcribed cDNA was subjected to 30–40 cycles of PCR amplification using the following primers *NOS*: 5'-GAAAAGAAGGGCCGAGATGTAT-3' and 5'- CAAGAGAAGGCAGATCATCAGC- 3'. The partial *NOS* cDNA fragment was cloned into the pGEM-T Easy vector (Promega) and verified by sequencing.

Digoxigenin-labeled RNA probes were synthesized by *in vitro* transcription using the DIG RNA Labelling Kit (Roche, Basel, Switzerland). The *NOS1* antisense probe was made by digestion of pGEM-T Easy vector: *NOS1* with *Sph*I and the sense probe by digestion with *Sal*I.

At day 10, ARs from five seedlings exposed or not to eBL 10^{-7} M, $As^{(III)}$, or $As^{(V)}$, alone or combined with eBL, were fixed in 70% (v/v) ethanol, embedded in paraffin, and sectioned at 8 μm with a Microm HM 350 SV microtome (Microm, Germany). The samples were treated with digoxigenin-labeled *NOS1* antisense and sense RNA probes overnight at 45 °C. *NOS1* mRNA detection was performed with 4-nitro blue tetrazolium chloride (NBT)/5-bromo-4-chloro-3-indolyl-phosphate (BCIP) overnight at room temperature according to Fornara et al. (2004). Sections were observed under light microscopy (Leica DMRB), and the absence of a hybridization signal in the sense probe-treated materials was also verified (Supplementary Figure 4).

2.6. Quantitative RT-PCR analysis of a putative OsNOS1 gene in rice roots

Total RNA was extracted from roots grown in the absence or presence of $As^{(III)}$ or $As^{(V)}$. RNAs for RT-PCR and real-time RT-PCR analyses were treated with RNase-free Dnase (Dnase I; PROMEGA) and reverse transcribed using SensiFAST cDNA Synthesis Kit (Bioline, London, UK), according to the manufacturer's instructions.

SYBR Green-based quantitative assays were performed in 10 μL of SensiFAST™ SYBR® No-ROX Kit (Bioline, London, UK) using LineGene 9620 qPCR detection system (Bioer, China).

The PCR conditions were: one cycle at 95 °C for 10 min, followed by 40 cycles at 94 °C for 15 s, 60 °C for 30 s, 72 °C for 30 s, and 1 cycle at 72 °C for 2 min. A dissociation cycle at 60 °C for 20 min was added at the end to check the specificity of the amplification reactions. The reactions were repeated three times with two different preparations of cDNA, and one representative experiment was plotted. Gene expression levels were normalized to the levels of *OsGAPDH* and *OsUBQ10* levels using the ΔΔCT method. The list of primers and the *NOS1* gene accession number are reported in Supplementary Table 1.

2.7. Statistical analysis

All the data were statistically analyzed using a one-way ANOVA test followed by Tukey's post-test (at least at $p < 0.05$) after having performed Shapiro–Wilk's normality test. The statistical analyses were carried out through GraphPad Prism (Version 9.3.0; GraphPad Software, San Diego, CA, USA) software. All the experiments were performed in three independent biological replicates with similar results. Data from the first or the second biological replicate are shown.

3. Results

3.1. A specific concentration of exogenous 24-epibrassinolide enhances lateral root formation in the presence of arsenate

To evaluate the possible mitigatory effects of BRs on rice root systems exposed to As, a morphological analysis was carried out on the roots of seedlings grown in the presence or not of $As^{(III)}$ or $As^{(V)}$ and with or without 24-epibrassinolide (eBL) at three different concentrations (10^{-6} M, 10^{-7} M or 10^{-8} M). Fig. 1 shows that eBL treatments affected the AR length in a concentration-dependent manner. Indeed, 10^{-6} M eBL had a significant inhibitory effect on AR length, which was reduced by 30.8% compared to the Control, while 10^{-7} M and 10^{-8} M eBL increased

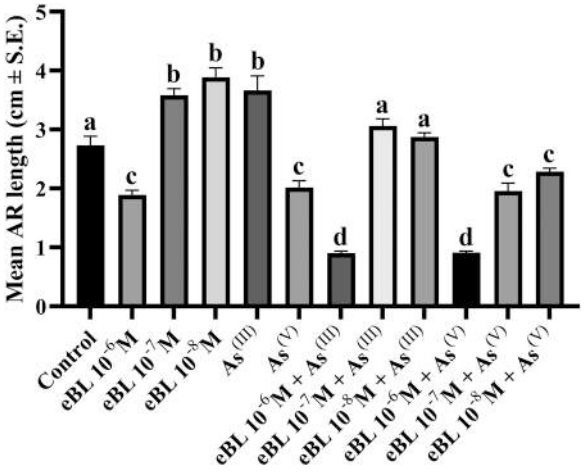

Fig. 1. Mean adventitious root (AR) length (± S.E.) of rice seedlings non-treated (Control) or treated with eBL at 10^{-6} M, 10^{-7} M, or 10^{-8} M combined or not with $As^{(III)}$ or $As^{(V)}$. Letters show significant differences for at least $p < 0.05$. The same letter shows no significant difference. Data from the second biological replicate. N = 30.

it by 31.2% and 42.2%, respectively ($p < 0.001$). The AR length was differently affected by the two As forms: $As^{(III)}$ increased AR length by 34.2% ($p < 0.001$) (Fig. 1), while $As^{(V)}$ reduced it by 26.2% ($p < 0.001$) (Fig. 1) in comparison with the Control. Moreover, the addition of 10^{-6} M eBL combined with either $As^{(III)}$ or $As^{(V)}$ caused a strong and significant ($p < 0.0001$) reduction of AR length (i.e., by 67% with respect to the Control) for both the As forms. The treatments with 10^{-7} M and 10^{-8} M eBL combined with $As^{(V)}$ did not change significantly the AR length, respect to the $As^{(V)}$ alone (Fig. 1), whereas when combined with $As^{(III)}$ they induced an AR elongation comparable to that of the Control ARs, but lower than what observed with $As^{(III)}$ alone (Fig. 1).

The treatments with 10^{-7} M or 10^{-8} M eBL, but not 10^{-6} M eBL, strongly increased the LR density (by 91% and 119% respectively) in comparison with the Control (Fig. 2). When applied alone, both the As species significantly and similarly reduced the LR density, by about 50%, with respect to the Control (Fig. 2). A total inhibition of lateral root primordia (LRPs) formation was observed when 10^{-6} M eBL was combined with $As^{(III)}$ (Fig. 2), while, the same eBL concentration in combination with $As^{(V)}$ did not affect LR density respect to $As^{(V)}$ alone (Fig. 2).

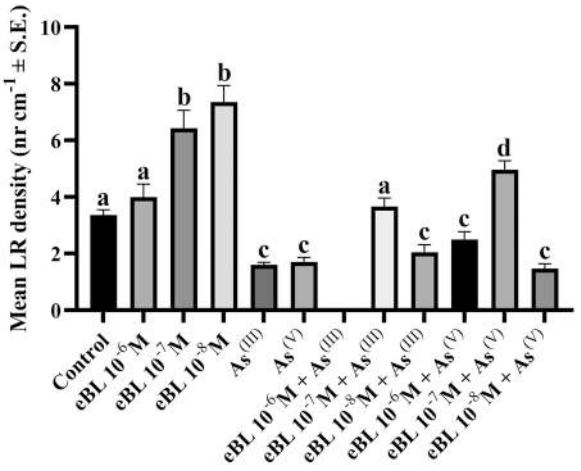

Fig. 2. Mean lateral root (LR) density (± S.E.) of rice seedlings non-treated (Control) or treated with eBL at 10^{-6} M, 10^{-7} M, or 10^{-8} M combined or not with $As^{(III)}$ or $As^{(V)}$. Letters show significant differences for at least $p < 0.05$. The same letter shows no significant difference. Data from the second biological replicate. N = 30.

Similarly, the combined treatment of 10^{-8} M eBL with $As^{(III)}$ or with $As^{(V)}$ did not significantly change the LR density in comparison with $As^{(III)}$ or $As^{(V)}$. By contrast, when 10^{-7} M eBL was combined with $As^{(III)}$ there was an increase ($p < 0.01$) in LR density by 129%, in comparison with $As^{(III)}$ alone, reaching values similar to the Control (Fig. 2). Interestingly, 10^{-7} M eBL combined with $As^{(V)}$ caused a relevant and highly significant ($p < 0.0001$) increase in LR density in comparison with the pollutant alone (i.e., by ~192%) and the Control (by ~47%) treatments ($p < 0.05$) (Fig. 2).

The highest eBL concentration strongly ($p < 0.0001$) reduced the fresh root system biomass by 40% compared to the Control (Fig. 3 and Supplementary Figure 3 A-B), while no significant change was observed with 10^{-7} M and 10^{-8} M eBL treatments (Fig. 3 and Supplementary Figure 3 C-D). The fresh root biomass was also significantly reduced by the exposure to both $As^{(III)}$ and $As^{(V)}$ treatments in comparison with the Control ($p < 0.0001$), by 29% and 25% respectively (Fig. 3 and Supplementary Figure 3 E-F). The highest eBL concentration, combined with either $As^{(V)}$ or $As^{(III)}$, further reduced ($p < 0.001$) the root biomass in comparison with either the Control or the metalloid alone (Fig. 3 and Supplementary Figure 3 G, J and A, E-F in comparison). Moreover, 10^{-7} M and 10^{-8} M eBL combined with either $As^{(III)}$ or $As^{(V)}$, did not significantly affect the root biomass with respect to the $As^{(III)}$ or $As^{(V)}$ alone treatments, thus not restoring the Control values (Fig. 3 and Supplementary Figure 3 H-I, K-L).

These results show that the eBL effects on the root system morphology are strictly concentration-dependent, with a positive effect on root development for the lowest concentrations. A similar trend was observed analyzing LR formation where 10^{-7} M eBL was the most effective concentration in alleviating $As^{(V)}$ toxicity.

Based on these results, the 10^{-7} M eBL concentration was chosen for the subsequent experiments aimed at a deeper understanding of the role of exogenous BRs in alleviating As stress in rice root-systems.

3.2. 24-epibrassinolide applied at 10^{-7} M does not mitigate the cytohistological damages induced by arsenite or arsenate, but reduces lignin deposition in the cell walls of the outermost cortical layers

Lateral and adventitious roots of seedlings treated or not with both the As forms and with 10^{-7} M eBL alone or combined with each of the two, were histologically analysed to verify if eBL was able to mitigate the toxic effects on the root anatomy caused by the pollutant (Fig. 4 and Fig. 5). In the roots, the exposure to toxic elements can alter the natural cellular barriers, such as the cell walls composition (Parrotta et al., 2015), to prevent toxic elements to reach the stele of the root from which they can get translocated to aerial organs. For this reason, lignin thickening in the cell walls of the sclerenchyma and of the outermost layers of the cortical parenchyma was analysed in ARs treated with both As forms, alone or in combination with eBL, and the lignin autofluorescence signal was quantified (Fig. 6).

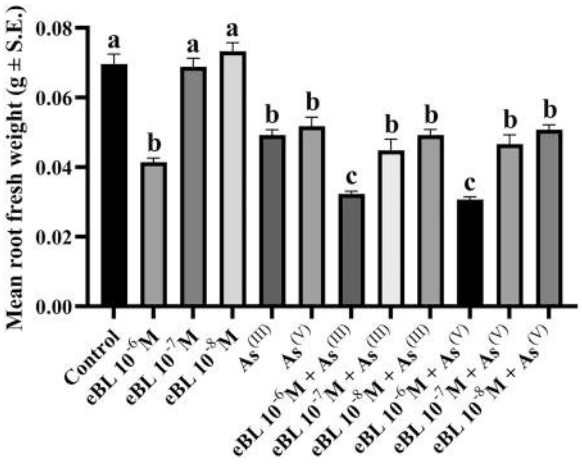

Fig. 3. Mean root fresh biomass (± S.E.) of rice seedlings non-treated (Control) or treated with eBL at 10^{-6} M, 10^{-7} M, or 10^{-8} M combined or not with $As^{(III)}$ or $As^{(V)}$. Letters show significant differences for least $p < 0.0001$. The same letter shows no significant difference. Data from the second biological replicate. N = 30.

In the Control, anticlinal divisions in the pericycle founder cells and in the endodermis of the ARs were the first steps of LRP formation and were followed by divisions into the three space dimensions, till complete formation of the root primordia (Fig. 4 A). The primordia development continued with the quiescent centre (QC) definition (Fig. 4 B, asterisks) in the root meristem stem cell niche, at VI–VII stages of LRP development (Ni et al., 2014), and the regular further longitudinal (Fig. 4 B) and radial growth (Fig. 4 C) of the root apex. In the mature ARs, tissues were regularly differentiated in the following order from the outside towards inside of the root: epidermis, exodermis, sclerenchyma layer, cortical parenchyma, endodermis, and vascular stele (Fig. 4 D). The analysis of lignin autofluorescence showed a slight signal in the cell walls of the sclerenchyma cells, and a still weaker signal in the walls of the outermost cortical parenchyma cells (Fig. 4 E, inset, and Fig. 6).

Arsenate, instead, altered LRP development, starting from the first cell divisions, with this leading to the formation of irregular LRPs (Fig. 4 F-G). These LRPs were characterized by the presence of differentiated cells even in the root meristem area, and by an irregular definition of the stem cell niche in it (Fig. 4 F, rectangle). Possibly depending on these anomalies, most of the LRPs failed to develop into elongated LRs. However, some primordia showed a quite regular organization (Fig. 4 H) and, therefore, developed into regular LRs. In the apical meristem, the main damages induced by $As^{(V)}$ were early cell differentiation (Fig. 4 I, arrows), accentuated meristematic cell vacuolization and early cell separation (Fig. 4 J, arrows). Transverse sections in the root primary structure region showed a complete tissue alteration of the differentiated tissues, with a hypertrophic parenchyma and a not properly differentiated endodermis (Fig. 4 J). Arsenate caused a slight, but not significant, increase of lignin deposition in the walls of the AR sclerenchyma cells, as well as an irregular, but highly significant ($p < 0.0001$), increase in the walls of the outermost cells of the cortical parenchyma, as measured by approx. 67% enhancement of lignin autofluorescence compared to the Control (Fig. 4 K, inset, E and Fig. 6).

The application of $As^{(III)}$ alone reduced LRP formation in comparison with the Control (Fig. 2). However, the few formed primordia were mostly able to develop properly (Fig. 4 L) showing only weak cytological alterations, mainly due to irregular cell divisions in the early phases of their formation (Fig. 4 M). Histological anomalies became more evident in the differentiated tissues where frequent plasmolysis in cortical cells (Fig. 4 N-O, arrows in N) and increased number of sclerenchyma cells, leading to a scattered bilayered sclerenchyma were observed (Fig. 4 P, arrows). As seen for $As^{(V)}$ treatment, also $As^{(III)}$ exposure induced a relevant ($p < 0.0001$) increase in the lignin deposition in the outermost cortical cells and, to a lesser extent, in the sclerenchyma cells, causing in ARs an overall ~53% increase in the autofluorescence signal compared to the Control (Fig. 4 Q and inset, and E in comparison, and Fig. 6).

Exogenous eBL induced an increase in LRP formation in comparison with the Control (Fig. 5 A, arrows, and Fig. 2). Primordia development occurred as observed in the Control: root domes were regularly defined, as well as the protoderm (Fig. 5 B-C, E). The elongated roots showed a regular apical meristem with a QC correctly positioned, a correct division pattern of the meristematic cells and a correct tissue differentiation (Fig. 5 D, E-F), even if sporadic differentiation events were also observed in the elongation zone (Fig. 5 D, arrow). Exogenous eBL did not significantly change lignin autofluorescence signal, neither in the sclerenchyma, nor in the outer layers of the cortical parenchyma, as compared to the Control (Fig. 5 G and 4 E in comparison, and Fig. 6).

When eBL was combined with $As^{(V)}$ no re-establishment of the normal development of the LRPs occurred (Fig. 5 H-J, and Fig. 4 F-J, in comparison). A widespread vacuolization of the meristematic cells was

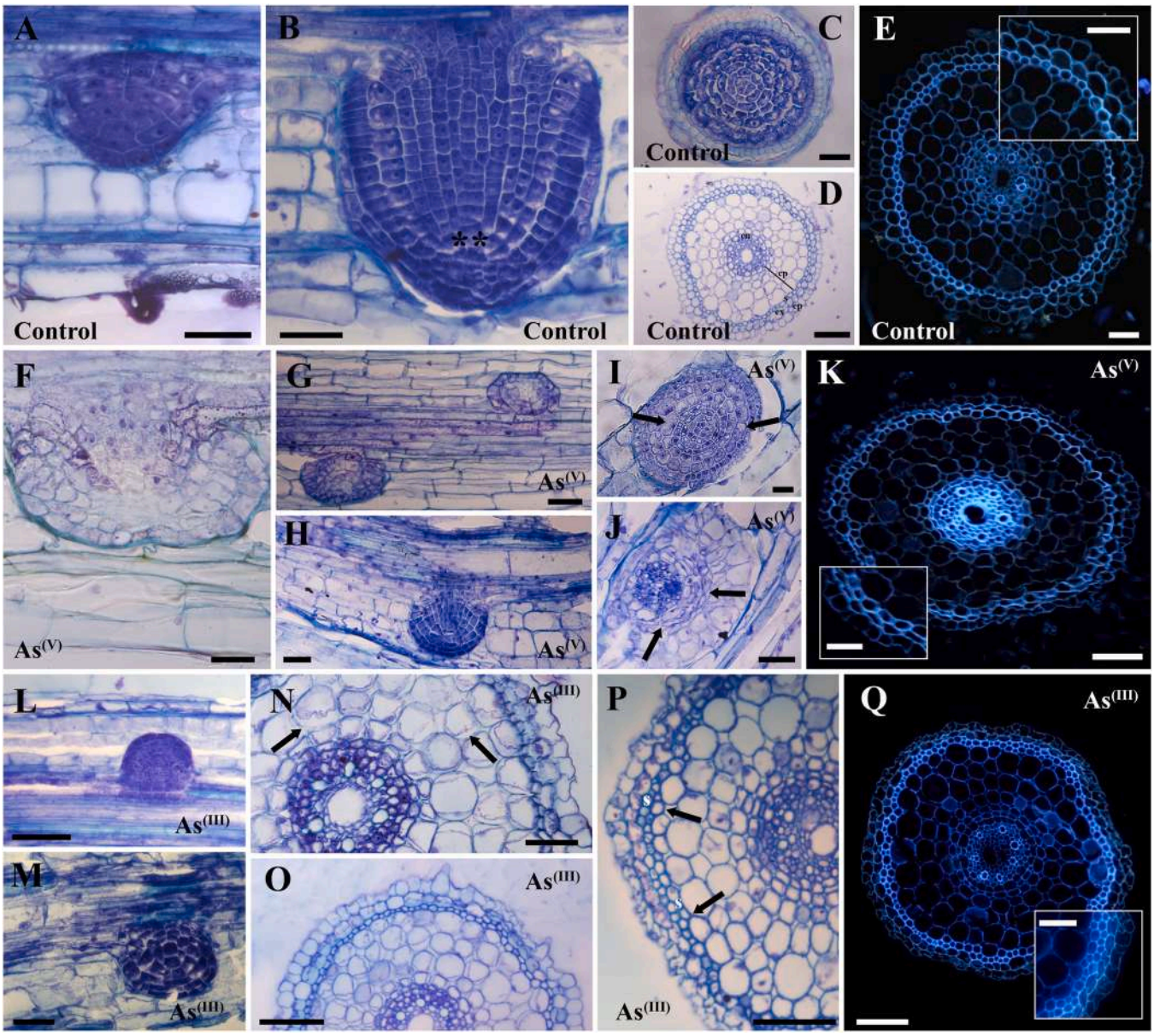

Fig. 4. Histological images of LRP, LR, and AR sections stained with toluidine blue and of AR sections showing lignin autofluorescence in rice seedlings non-treated (Control) (**A-E**) or treated with $As^{(V)}$ (**F-K**) or $As^{(III)}$ (**L-Q**). Images from the first and second biological replicates. Bars = 50 μm (A, B, E, F, I, M, inset in E), 100 μm (C, D, G, H, J, L, N-P, insets in K and Q), 200 μm (K, Q). cp, cortical parenchyma; en, endodermis; ep, epidermis; ex, exodermis; s, sclerenchyma.

present, as already observed in the earliest developmental stages of the root dome (Fig. 5 H, arrow), as well as an incorrect definition of the QC at stage VII of primordium development (Fig. 5 I, asterisks), and the presence of LRPs with differentiated cells instead of meristematic cells and no proper dome (Fig. 5 J). The differentiating tissues of the elongated roots also showed strong anomalies, such as an early formation of the aerenchyma, hypertrophy of the cortex, and an altered differentiation of the tissues inside the stele (Fig. 5 K-L arrows).

Interestingly, the supplementation of eBL together with $As^{(V)}$ reduced lignin deposition in the sclerenchyma cell walls, but especially in the outermost cortical cells walls of the ARs, respect to the pollutant alone (Fig. 5 M). This was confirmed by an approximately 45% reduction in the lignin signal of the cortical parenchyma, which became similar to that of the Control (Fig. 5 M and 4 E in comparison, and Fig. 6).

The combination of eBL with $As^{(III)}$ did not restore the correct histological organization of roots. On the contrary, the damages induced by $As^{(III)}$ were further increased by eBL presence, even if the root primordia showed reduced alterations (Fig. 5 N-O). Major damages were detected instead in the root primary structure region. High hypertrophy and plasmolysis in the cortical cells, increased aerenchyma formation, and increased thickness of the sclerenchyma (Fig. 5 P, R, arrows, and Fig. 4 N-P, in comparison) were observed. However, as in the case of eBL combined with $As^{(V)}$, the combination of the eBL with the $As^{(III)}$ reduced the production of lignin with respect to the $As^{(III)}$ alone (i.e., by ~54% in the cortical parenchyma and by ~18% in the sclerenchyma), thereby reducing the autofluorescence signal up to the Control values (Fig. 5 Q and 4 E, in comparison, and Fig. 6).

Thus, the cyto-histological analysis shows that eBL, at the concentration of 10^{-7} M, is unable to reduce the histological damages induced by both the As species in the LRs and ARs. However, the BR has a positive and tissue-specific effect, because it counteracts the deposition of lignin in the cell walls of the cortical parenchyma, event which is instead strongly induced by both the As species.

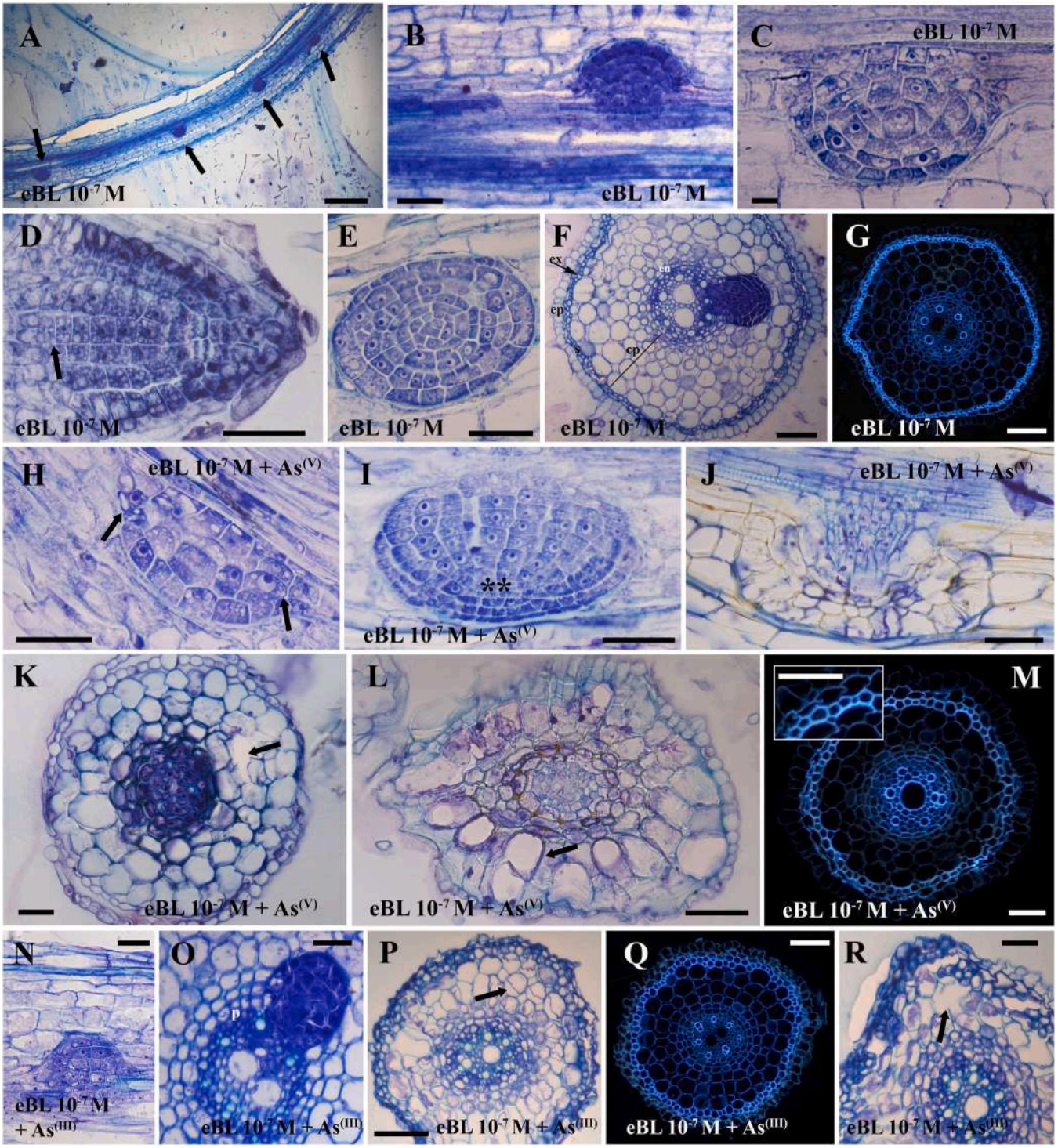

Fig. 5. Histological images of LRP, LR, and AR sections stained with toluidine blue and of AR sections showing lignin autofluorescence in rice seedlings treated with eBL at 10^{-7} M alone (**A-G**) or combined with $As^{(V)}$ (**H-M**) or $As^{(III)}$ (**N-R**). Images from the first and second biological replicate. Bars = 50 μm (B, C, H, J, K, O, R), 100 μm (D-F, I, L, M, N, P, inset in M), 200 μm (G, Q), 600 μm (A). cp, cortical parenchyma; en, endodermis; ep, epidermis; ex, exodermis; p, pericicle; s, sclerenchyma.

3.3. 24-epibrassinolide at 10^{-7} M enhances NO levels in the rice roots and restores its level and cellular distribution both altered by arsenate

To verify if the eBL treatments induced changes in NO distribution/accumulation, root systems composed of ARs, LRs, and LRPs of seedlings grown in the presence of $As^{(III)}$ or $As^{(V)}$ or eBL 10^{-7} M, alone or combined with each of the two As species, were incubated with the NO-specific fluorescence probe DAF-FM DA, and the epifluorescence signal monitored and quantified (Fig. 7). In the Control treatment, the NO signal was mainly localized in the root cap, in the root differentiation zone, in the outermost tissues of the mature ARs confining with the LRPs, and weakly in the primordia (Fig. 7 A-C). The treatment with eBL induced a very strong (about 69% increase compared to the Control, $p < 0.0001$) NO signal in all root types, without changing the signal localization in

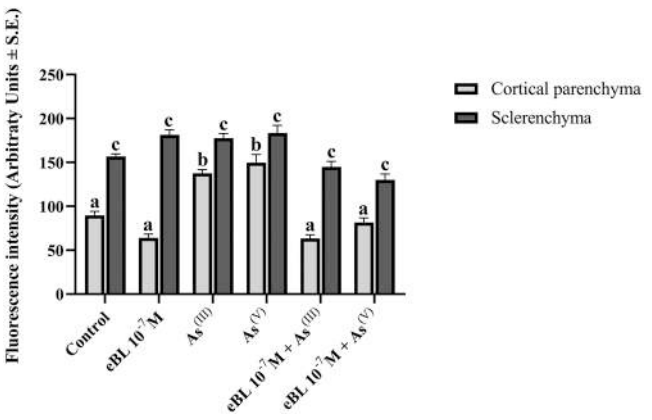

Fig. 6. Mean intensity (± S.E.) of lignin autofluorescence expressed in arbitrary units using ImageJ software in the cells of outermost cortical parenchyma (light-grey bars) and in the sclerenchyma cells (dark-grey bars) of ARs non-treated (Control) or treated with eBL at 10^{-7} M combined or not with $As^{(III)}$ or $As^{(V)}$. Data from the second biological replicate. Letters show significant differences for at least $p < 0.01$ within the same tissue. The same letter shows no significant difference. N = 60 (see materials and methods Section).

comparison with the Control (Fig. 7 D-F and A-C in comparison, and S).

Both $As^{(III)}$ and $As^{(V)}$ reduced the NO signal, and by ~10% and ~55% compared to the Control, respectively (Fig. 7 G-L and A-C). However, the decrease in fluorescence intensity was quantitatively significant ($p < 0.001$) only in the presence of $As^{(V)}$ (Fig. 7 S). Moreover, the $As^{(V)}$ treatment also modified the intracellular NO distribution in the ARs, in comparison with the Control, because a higher number of the meristematic cells, and a smaller number of the cap cells showed signal in the apex (Fig. 7J and A in comparison). The eBL 10^{-7} M combined with $As^{(III)}$ further reduced by ~30% signal intensity with respect to the Control, although not significantly (Fig. 7 M-O and A-C, S). In addition, a fluorescence signal was occasionally evident in the meristematic zone of LRs (Fig. 7 O). On the contrary, when 10^{-7} M eBL was combined with $As^{(V)}$, the signal intensity significantly ($p < 0.001$) increased by 110% in comparison with the metalloid alone, reaching values comparable to those of the Control both in terms of intensity and localization pattern (Fig. 7 P-R and A-C, S).

Altogether, the results of NO epifluorescence analysis show that the exogenous eBL at 10^{-7} M concentration induces a strong NO increase compared with the Control, thus maintaining, at the same time, its distribution pattern in the root. By contrast, $As^{(V)}$ reduces the NO signal, by altering also its cellular distribution, but the exogenous eBL restores the NO levels and its distribution pattern in the root cells.

3.4. Exogenous 24-epibrassinolide at 10^{-7} M enhances OsNOS1 gene expression in the roots even when combined with arsenite or arsenate

To verify if the BR and As induced NO synthesis through *NOS* gene expression, an *in situ* hybridization analysis of the putative *OsNOS1* gene was performed in ARs and LRs non-exposed or exposed to eBL (10^{-7} M), $As^{(III)}$ and $As^{(V)}$ alone or in combination. Preliminary, changes in the expression of the *OsNOS1* gene caused by either As species in the rice roots were verified by a qRT-PCR analysis (Supplementary Figure 2).

In the Control roots, gene transcript levels were weak and mainly localized in the epidermis and in the parenchyma cells associated with the ARs vascular system, in the cells of LRPs at the initial stages (Fig. 8 A-B), and in all the meristematic cells of the LR apices (Fig. 8 C).

Arsenate significantly ($p < 0.001$) increased gene transcript expression in comparison with the Control (Supplementary Figure 2). In the mature roots, the signal was mainly localized in the epidermal cells (Fig. 8 D-E) and at the base of LRs (Fig. 8 F). In the elongation region of the LRs the cells destined to differentiate into sclerenchyma also showed a strong gene expression (Fig. 8 G, arrows). On the contrary, the cells of the primordia altered by $As^{(V)}$ showed only a weak *OsNOS1* transcript signal (Fig. 8 H).

Arsenite induced a significant ($p < 0.01$) reduction of *OsNOS1* expression in comparison with the Control and $As^{(V)}$ (Supplementary Figure 2). The *in situ* hybridization confirmed the very low signal of the gene transcripts, both in mature AR tissues (Fig. 8 I) and in the meristematic cells of the forming LRPs (Fig. 8 J-L).

The treatment with 10^{-7} M eBL strongly increased *OsNOS1* transcription levels in comparison with the Control both in the cells of the mature ARs, such as epidermal cells and parenchyma cells associated with the vascular tissues, and in those of the forming LRPs (Fig. 9 A-D and Fig. 8 A-C, in comparison). When eBL was combined with either $As^{(III)}$ or $As^{(V)}$, the signal was very strong and localized in the cells of both mature ARs and LRs and in cells of LRPs (Fig. 9 E-H, I-L). Interestingly, the BR combination of eBL with $As^{(III)}$ reinforced the signal in the cortical cells of the ARs (Fig. 9 I) as well as inside the stele (Fig. 9 K), and in the LRPs (Fig. 9 J) in comparison with the Control and with $As^{(III)}$ alone (Fig. 9 I-L and Fig. 8 A-C and I-L in comparison).

The absence of a hybridization signal in ARs and LRs exposed or not to eBL and $As^{(V)}$ or $As^{(III)}$, alone or together, was verified with the sense probe, as shown in Supplementary Figure 4.

Overall, the expression of the *OsNOS1* gene reveals that $As^{(V)}$ alone induces the gene overexpression, while $As^{(III)}$ decreases it, compared with the Control, and that eBL alone significantly increases *OsNOS1* gene expression, with an additive effect when combined with both As forms.

4. Discussion

The results show that eBL affects the morphology of rice root systems depending on its concentration, with a specific level (10^{-7} M) being the most effective for development. This eBL concentration is also the most effective in relieving As toxicity in this plant. However, it does not reduce As-induced damages in the LRs and ARs, even if it is able to counteract lignin deposition in the cell walls of the cortical cells. This indicates that 10^{-7} M eBL has a precise effect on the cell wall, which is at the same time target and barrier in the first responses of the plant cells to the toxicity of environmental pollutants.

Moreover, $As^{(V)}$ reduces the NO signal in ARs and LRs, and alters its cellular distribution. On the contrary, eBL alone increases NO levels and maintains its regular distribution pattern when applied alone. Interestingly, eBL restores NO levels and the tissue distribution also when combined with $As^{(V)}$.

For the first time here, the tissue localization of *OsNOS1* transcripts in rice ARs and LRs is shown revealing that the expression of this gene is strongly dependent on the presence of both As forms and of eBL. More precisely, $As^{(V)}$ induces the overexpression, whereas $As^{(III)}$ reduces the expression of *OsNOS1*. Also, the eBL alone increases this gene expression, but mainly when combined with $As^{(III)}$ or $As^{(V)}$.

4.1. Brassinosteroids improve the morphology of root systems even in the presence of arsenic, and reduce the physical barrier due to lignin deposition in the walls of the cortical cells

The metalloid Arsenic, in its inorganic forms of $As^{(III)}$ and $As^{(V)}$, is one of the most worrying environmental pollutants. Arsenate, being a phosphate analog competes with phosphate during phosphorylation reactions and alters phosphate metabolism during ATP synthesis and phosphorylation (Farooq et al., 2022) causing cell oxidative stress, and reduced root growth (Ronzan et al., 2018). Arsenite, instead, binds to the sulfhydryl groups of enzymes and proteins causing a modification of their structure and activity (Farooq et al., 2022). Protein that are known to bind $As^{(III)}$ include transcription factors, signal transduction proteins, proteolytic proteins, metabolic enzymes, redox regulatory enzymes, and structural proteins (Finnegan and Chen, 2012, and references therein).

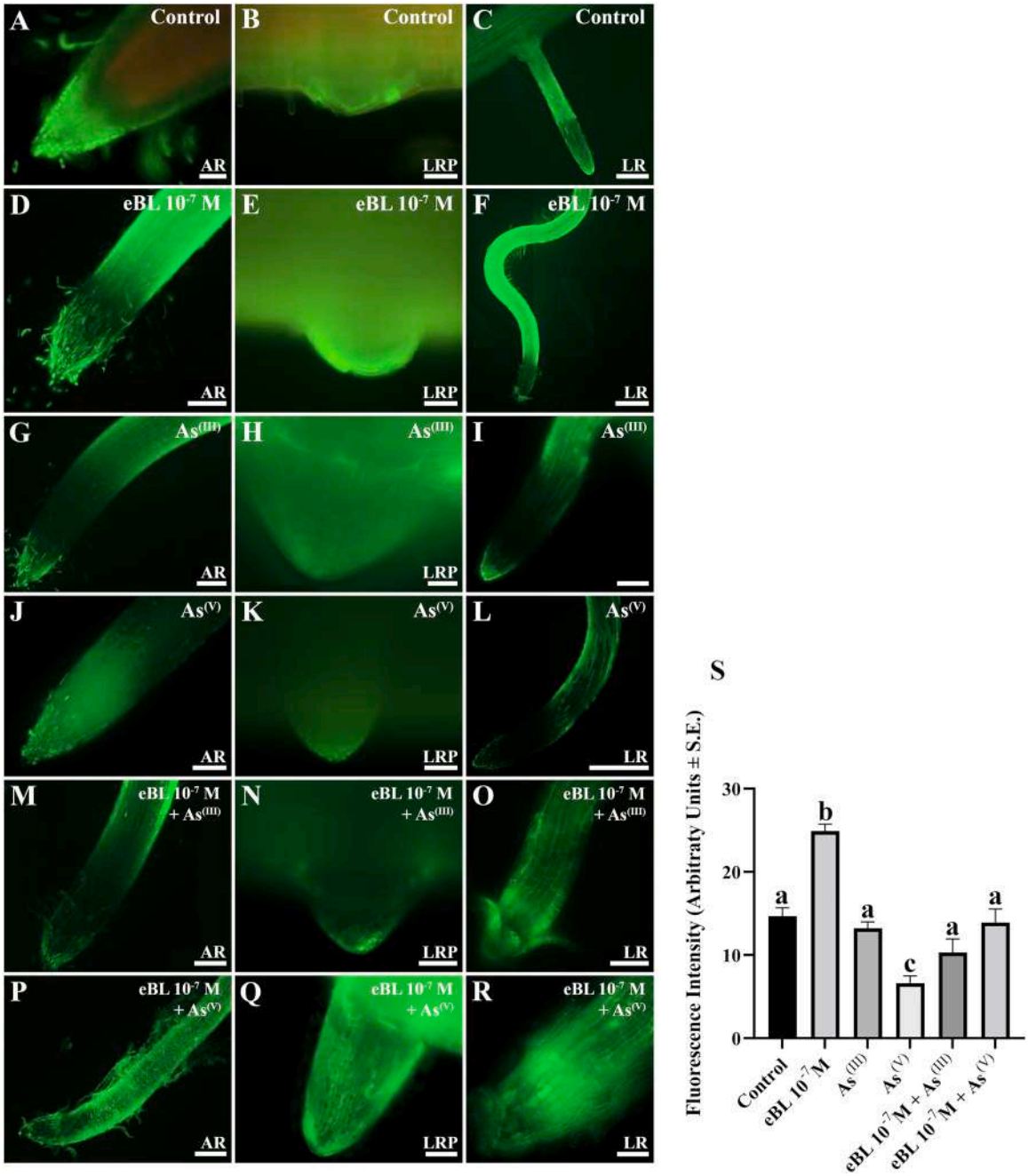

Fig. 7. NO fluorescence signal in the root system (ARs, LRs, and LRPs) from 10-days-old rice seedlings non-treated (Control, **A-C**) or treated with eBL 10^{-7} M alone (**D-F**) or combined with $As^{(III)}$ (**M-O**) or $As^{(V)}$ (**P-R**). Bars = 25 μm (H, Q, and R), 50 μm (A, B, E, I-K, N, and O), 100 μm (C, D, G, M, and P), 600 μm (F and L). Nitric oxide fluorescence quantification in ARs and LRs using Zen 2.5 image analysis software (Zeiss) (**S**). Data and images from the second biological replicate. Letters show significant differences for at least $p < 0.01$. The same letter shows no significant difference. N = 10 (see materials and methods section).

Moreover, As also alters membrane permeability and selectivity in root cells reducing the uptake of nutrients (Gusman et al., 2013). This strongly affects the development of the root system compromising its functionality, as previously reported (Lou et al., 2015; Ronzan et al., 2018; Piacentini et al., 2020a) and confirmed by the results of this work. However, the plant root systems are highly plastic in response to environmental stimuli, including the presence of toxic elements, to allow adaptation to altered conditions and plant survival.

The root system plasticity is ensured by the involvement of different phytohormones. In fact, phytohormones, including BRs, a class of steroidal compounds, represent the interface between external stimuli and the activation of the plant defense responses (Zluhan-Martínez et al., 2021). The results here presented show that exogenous eBL, one of the most biologically active BRs, regulates root architecture, increasing the LR formation and development in a dose-dependent manner, similarly to what happens in maize root systems under different BR concentrations and growth conditions (Zhang et al., 2022). It was proposed that BRs interact with other phytohormones, mainly auxin, for inducing LR formation and for maintaining the correct organization and functionality of the roots (Ackerman-Lavert et al., 2021). Indeed, *ZmIAA2* and *ZmIAA30* maize genes, homologous to Arabidopsis *IAA14* and *IAA28* genes, which code for factors inhibiting LRP formation, are down-regulated by BR treatments. On the contrary, *ZmARF7* and *ZmARF19* genes, coding for factors promoting LRP formation, are up-regulated by BRs (Zhang et al., 2022, and references therein). Root systems are fibrous in rice, as in maize, and the Aux/IAA and ARF proteins control root architecture in

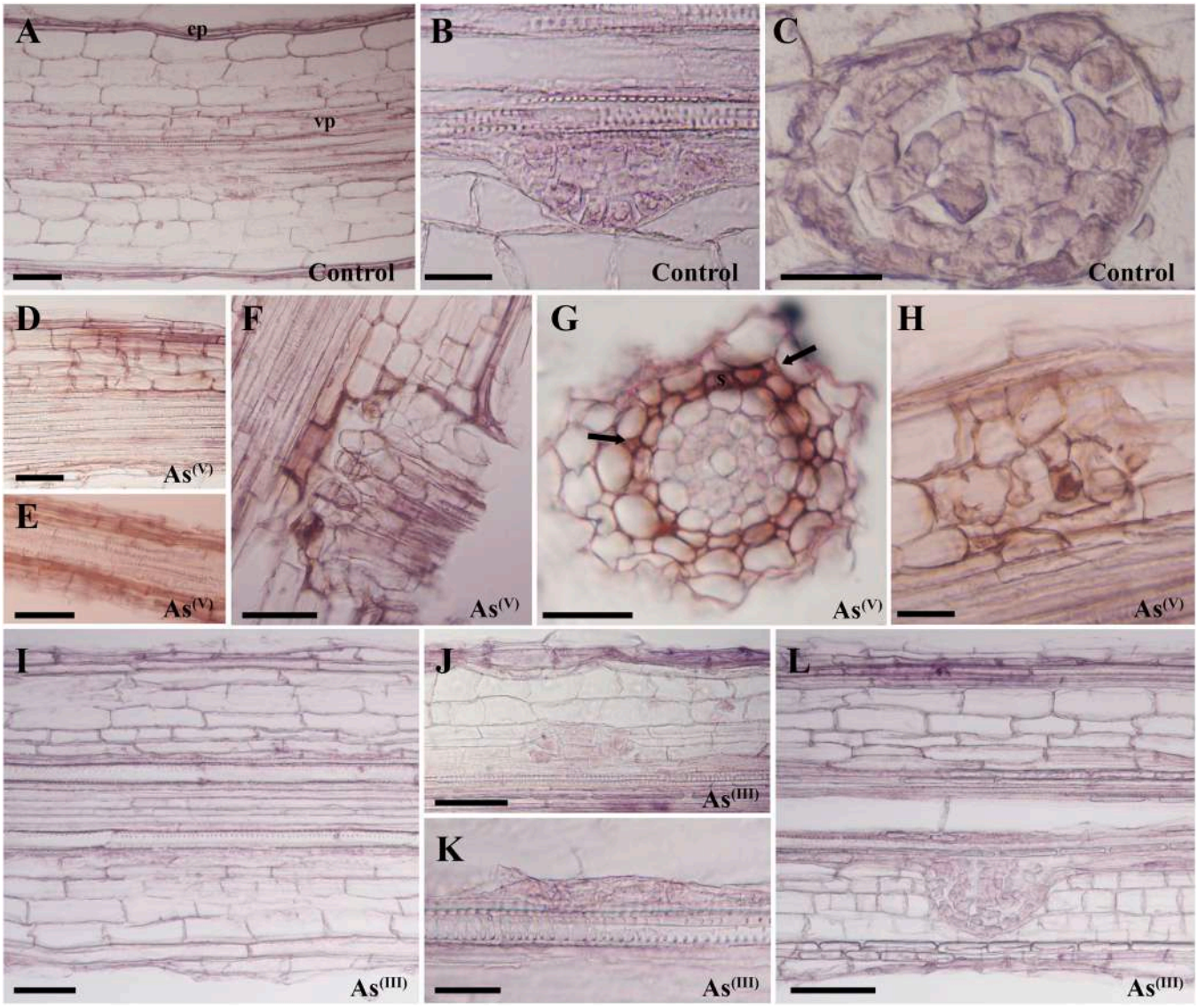

Fig. 8. *In-situ* hybridization of *OsNOS1* in rice LRPs, LRs, and ARs not treated (Control; **A-C**) or treated with $As^{(v)}$ (**D-H**) or $As^{(III)}$ (**I-L**). Images from the second biological replicate. Bars = 25 μm (B, C, F, H), 50 μm (A, D, G, L), 100 μm (E). ep, epidermis; s, sclerenchyma; vp, vascular parenchyma.

both plants (Liscum and Reed, 2002). Thus, it is possible that the same interaction between auxin and BRs is active also in the control of LRP formation of rice, and through the same proteins.

Evidences show that BRs also play a positive role in stabilizing the root systems of plants exposed to stressful environmental conditions through interactions with auxin and other hormones (Devi et al., 2022). The protective role of BRs under stress conditions also emerges from our results. However, the histological results show that the BRs are unable to alleviate some cellular damages in the ARs and their LRPs, and especially those occurring at the very early stages of LRP formation. In fact, both the As forms inhibit the regular formation of the QC and the stem cell niche around it in the LRPs, thereby preventing their development into elongated roots, and BRs are unable to restore the normal QC definition and the regular further growth. It is possible that, in rice, exogenously applied BRs, at the concentration used in this research, combined with a strong stressor, such as inorganic As, are not able to control the root stem cell niche definition, renewal and maintenance, which depend by a functional QC, contrarily to what happens in Arabidopsis roots developed in physiological conditions (Vilarrasa-Blasi et al., 2014). However, the activation of stress-associated BR-signalling causes an increase in QC divisions and premature stem cell differentiation also in the stem cell niche of Arabidopsis roots, resulting in anomalous root growth (González-García et al., 2011; Heyman et al., 2013). In accordance, we show that As, alone or combined with eBL, causes an alteration of cell division planes in the early stages of LRP development and that the eBL is unable to reverse this anomaly. In the absence of eBL, Ronzan and co-workers (2018) reported the same anomalies in rice roots after exposure to cadmium and $As^{(V)}$, alone or combined each other. Toxic elements can inhibit cell divisions by disrupting the cytoskeleton, targeting microtubules and microfilaments (Horiunova et al., 2016). It is, therefore, possible that also As has the same effects on cytoskeletal components. In Arabidopsis, it is also known that BRs stabilize the cytoskeleton by interacting with auxin (Lanza et al., 2012). Auxin is responsible of stem cell niche and QC definition/maintenance in all root types of Arabidopsis (Della Rovere et al., 2013, and references therein) and rice (Yang et al., 2017), and of the regulation of cell division orientation by cytoskeleton (Vaddepalli et al., 2021). Under our experimental conditions, it is possible that the strong toxicity of As does not allow BRs to restore the normal cytoskeletal activity during cell divisions, probably because their interaction with auxin is disturbed, leading to irregular cell divisions in the LRPs.

It has been reported that inorganic As increases lignin deposition in

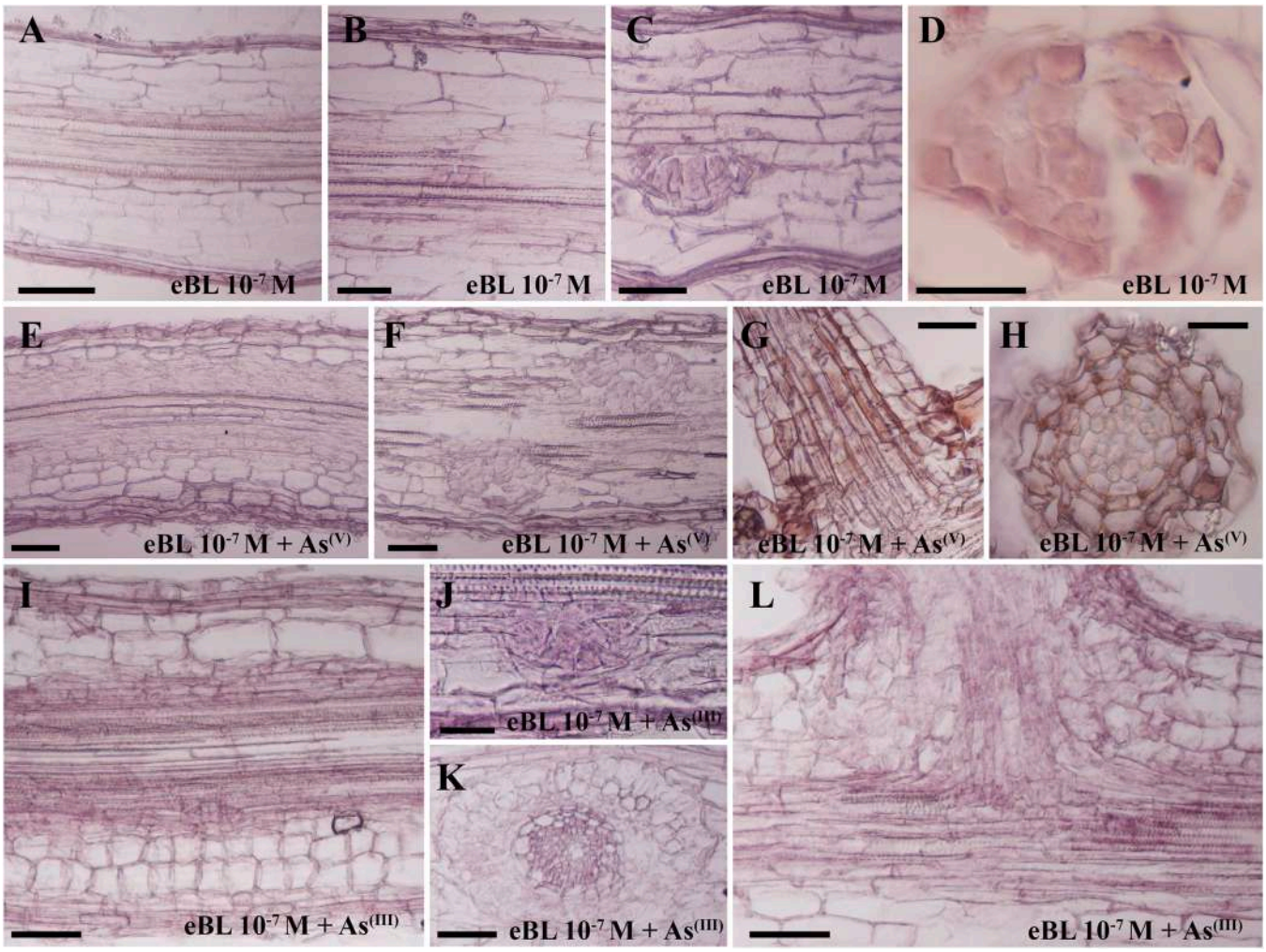

Fig. 9. *In-situ* hybridization of *OsNOS1* in rice LRPs, LRs, and ARs grown in the presence of eBL 10^{-7} M alone (**A-D**) or combined with $As^{(V)}$ (**E-H**) or $As^{(III)}$ (**I-L**). Images from the second biological replicate. Bars = 25 μm (B, C, F, G), 50 μm (A, D, H-L), 100 μm (E).

the cell walls of sclerenchyma cells in rice roots exposed to cadmium, $As^{(V)}$ or other heavy metals, suggesting that this is a plant strategy to limit the entry of heavy metal/metalloid into the internal root tissues (Moura et al., 2010; Piacentini et al., 2020a). Interestingly, the present results show that the two forms of As induce a thickening of the cell walls, by an increased lignin deposition, but this mainly occurs in the outer layers of the cortical parenchyma. Considering that the lignin biosynthesis depends on stress intensity (Cesarino, 2019), the response of the cortical parenchyma demonstrates that this process is involved in the adaptation to a strong As toxicity. In fact, it shows how the plant modifies the cells of a tissue which performs other functions in physiological/unstressed conditions, as accumulation of reserves, transforming it into a protective barrier to hinder the movement of the toxic element. In accordance, the overexpression of the rice peroxidase gene *OsPRX38* in *Arabidopsis thaliana* reduces As accumulation and causes lignin deposition in the apoplasts strengthening the concept that lignin deposition acts as a barrier for As entry via the root (Kidwai et al., 2018).

Treatments with eBL, alone or combined with each of the two As forms, does not substantially modify the deposition of lignin in the cell walls of sclerenchyma, which is a tissue normally committed to strengthen the root, but significantly reduce it in the cell walls of cortical parenchyma, a tissue with a more plastic development. In monocots, BRs have been reported to be involved in cell wall remodelling by regulating the expression of several genes encoding BR-mediated cell wall loosening proteins in response to abiotic stresses (Rao and Dixon, 2017). It is, therefore, possible that, in the presence of a metalloid stress providing an input of lignin biosynthesis in cells not usually committed to synthesize lignin, as in the cortical parenchyma cells, BRs activate processes reducing the compactness of the cell wall and the lignin deposition, thus allowing cortical cells to restore their normal functions. Therefore, BRs could play a positive role on the root systems in the presence of the pollutant by mitigating an excessive production of lignin that could compromise the root growth and survival.

4.2. Nitric oxide is configured as a key intermediary in the BR-mediated responses of rice root systems to arsenic stress

It is known that the endogenous metabolism of ROS and RNS is significantly affected by the activation of nitro-oxidative pathway in As-stressed plant cells (Bhat et al., 2021). Among the reactive nitrogen species, NO plays an essential role in plant responses to abiotic stresses modulating the cellular antioxidant enzyme system (Meng et al., 2022). Present data show that $As^{(III)}$ does not substantially modify NO levels in rice ARs and LRs, compared to the Control, whereas $As^{(V)}$ significantly reduces them and modifies the intracellular distribution of NO. It is known that NO activates the expression of ABC transporters (Grün et al., 2006), thus increasing the vacuolar sequestration of $As^{(III)}$-phytochelatin complexes (Song et al., 2014) in the roots and partially inactivating $As^{(III)}$ toxic effects. The vacuolar sequestration has not been shown for $As^{(V)}$. Thus, $As^{(V)}$ is free to move and could activate oxidative damage, thereby negatively impacting on NO levels/distribution.

It is known that part of $As^{(V)}$ is reduced to $As^{(III)}$ in the root cells, but

it is also possible that part of $As^{(III)}$ gets re-oxidated to $As^{(V)}$ (Zvobgo, 2022), and that $As^{(V)}$ is loaded into xylem vessels by the phosphate transporters (Mendoza-Cózatl et al., 2011). This could explain the observed inhibitory effect of $As^{(V)}$ on the NO signal reduction and alteration in distribution in ARs and LRs, but also on the reduction in AR elongation. To sustain this, it has been very recently demonstrated that $As^{(V)}$ reduces the length of rice ARs much more than $As^{(III)}$, albeit in a dose and a cultivar-dependent manner (Mondal et al., 2022).

We have previously shown that NO is unable *per se* to alleviate As-induced damage in rice roots (Piacentini et al., 2020a). However, considering that exogenous eBL strongly increases NO synthesis and that some damages, such as reduced LRs density and increased thickness of cortical parenchyma cell walls, are reversed by combined treatments of eBL and As, it is possible that NO participates in the mechanisms triggered by the eBL to relieve the stress caused by both the As forms in rice roots.

The specific mechanism of BR/NO interaction is still poorly understood (Altamura et al., 2023). However, there is evidence that BRs could regulate NO levels in Arabidopsis LR formation by inducing *Nitrate reductase* (*NR*) and *NO Synthase* (*NOS*)- like genes (Hu et al., 2021, and references therein). Yet, also NO can modulate BR levels. In fact, transcription factors leading to the expression of genes involved in BR-regulated processes are induced by NO (Castillo et al., 2018; Altamura et al., 2023).

In the present work, we also show that eBL alone significantly enhances NO levels in the rice roots, and that, when combined with As [mainly $As^{(V)}$], it restores NO levels and its cellular distribution. In accordance, in *Cucumis sativus* exogenous treatments with BRs induce endogenous NO synthesis probably to promote AR formation, and in *Arabidopsis thaliana* they restore root architecture (Tossi et al., 2013; Li et al., 2020). It is possible that also in rice root systems exposed to $As^{(V)}$-stress, in particular, the NO synthesis induced by exogenous eBL is activated to relieve the toxic effects of the metalloid. Thus, the BR action in relieving As stress in rice roots might have NO as a mediator.

It was reported that BRs promote an increase in NO levels by involving both nitrate/nitrite reductase pathway and NOS-like activities (Bhat et al., 2021, and references therein). Here we show that a NOS activity, specifically the activity of OsNOS1, plays a prevalent role in the synthesis of NO, especially in the presence of As. At our knowledge, this is the first time that the cellular localization of *OsNOS1* gene transcripts is shown in rice root tissues. Furthermore, here it is shown that eBL alone, and especially when combined with each of the two forms of As, enhances the signal of the gene transcripts in *in situ* hybridization experiments. In addition, by comparing the localization of NO accumulation sites, i.e., epidermis of mature ARs and LRs, the root stele and the early LRPs, with the sites where the *OsNOS1* transcripts signal is more evident, a strong similarity emerges. However, since NO is produced in plant cells through a variety of ways, including oxidative, reductive, and non-enzymatic reactions (Meng et al., 2022), further analyses are needed to shed full light on NO biosynthetic pathways in plants, under stress conditions in particular.

5. Conclusion

The results show that a specific concentration of exogenous eBL improves the morphology of rice root systems in the presence of As, and that NO is a key mediator in the BR-induced responses to this pollutant. These results increase the knowledge on the mechanisms of action of BRs in protecting the plants from the stress induced by toxic elements and pave the way to applications of these phytohormones in the cultivation of agronomically important plants such as rice, which may be highly subject to As-contamination.

Fundings

The authors acknowledge the financial support provided by the Sapienza University of Rome, grant numbers RM12117A5198B688 to FG and MISE Programma Operativo Nazionale "Imprese e Competitività" 2014-2020 FESR, nr. F/200088/01-03/X45 to AMM.

CRediT authorship contribution statement

P.D.: Conceptualization, Data curation, Formal analysis, Investigation, Methodology, Writing – original draft. **D.R.F.:** Investigation, Data curation. **L.F., C.M. and P.M.:** Histological Methodology. **F.L.:** Investigation, Data curation. **C.V.:** Molecular Methodology. **A.M.M.:** Conceptualization, Data elaboration, Writing. **F.G.:** Conceptualization, data elaboration, Writing – review & editing.

Declaration of Competing Interest

The authors declare that they have no known competing financial interests or personal relationships that could have appeared to influence the work reported in this paper.

Data Availability

Data will be made available on request.

Acknowledgments

We are grateful to Dr.ssa Raffaele G., Dr. Roscignoli G. and Sig. Cerioni C. for technical support in the analyses of *OsNOS1* gene expression and to Dr.ssa Betti C. (University of Milan) for the revision of the English language. Research was funded by the Sapienza University of Rome, grant numbers RM12117A5198B688 to FG and by MISE Programma Operativo Nazionale "Imprese e Competitività" 2014–2020 FESR, nr. F/200088/01–03/X45 to AMM.

Appendix A. Supporting information

Supplementary data associated with this article can be found in the online version at doi:10.1016/j.envexpbot.2023.105287.

References

Abbas, G., Murtaza, B., Bibi, I., Shahid, M., Niazi, N.K., Khan, M.I., Amjad, M., Hussain, M., Natasha, 2018. Arsenic uptake, toxicity, detoxification, and speciation in plants: physiological, biochemical, and molecular aspects. Int. J. Environ. Res. Public. Health 15 (59). https://doi.org/10.3390/ijerph15010059.

Ackerman-Lavert, M., Fridman, Y., Matosevich, R., Khandal, H., Friedlander-Shani, L., Vragović, K., Ben El, R., Horev, G., Tarkowská, D., Efroni, I., Savaldi-Goldstein, S., 2021. Auxin requirements for a meristematic state in roots depend on a dual brassinosteroid function. e6 Curr. Biol. 31, 4462–4472. https://doi.org/10.1016/j.cub.2021.07.075.

Altamura, M.M., Piacentini, D., Della Rovere, F., Fattorini, L., Falasca, G., Betti, C., 2023. New paradigms in brassinosteroids, stringolactones, sphingolipids, and nitric oxide interaction in the control of lateral and adventitious root formation. Plants 12, 413 https://doi.org/103390/plants12020413.

Anwar, A., Liu, Y., Dong, R., Bai, L., Yu, X., Li, Y., 2018. The physiological and molecular mechanism of brassinosteroid in response to stress: a review. Biol. Res. 51, 46. https://doi.org/10.1186/s40659-018-0195-2.

Beemster, G.T.S., Baskin, T.I., 1998. Analysis of cell division and elongation underlying the developmental acceleration of root growth in *Arabidopsis thaliana*. Plant Physiol. 116, 1515–1526 https://doi/10.1104/pp.116.4.1515.

Betti, C., Della Rovere, F., Piacentini, D., Fattorini, L., Falasca, G., Altamura, M.M., 2021. Jasmonates, ethylene and brassinosteroids control adventitious and lateral rooting as stress avoidance responses to heavy metals and metalloids (https://doi.org/doi:). Biomolecules 11 (77). https://doi.org/10.3390/biom11010077.

Bhat, J.A., Ahmad, P., Corpas, F.J., 2021. Main nitric oxide (NO) hallmarks to relieve arsenic stress in higher plants. J. Hazard. Mater. 406, 124289 https://doi.org/10.1016/j.jhazmat.2020.124289.

Cao, X., Zhu, C., Zhong, C., Zhang, J., Wu, L., Jin, Q., Ma, Q., 2019. Nitric oxide synthase-mediated early nitric oxide burst alleviates water stress-induced oxidative damage in ammonium-supplied rice roots. BMC Plant Biol. 19, 108. https://doi.org/10.1186/s12870-019-1721-2.

Castillo, M.C., Coego, A., Costa-Broseta, A., León, J., 2018. Nitric oxide responses in Arabidopsis hypocotyls are mediated by diverse phytohormone pathways. J. Exp. Bot. 69, 5265–5278. https://doi.org/10.1093/jxb/ery286.

Cesarino, I., 2019. Structural features and regulation of lignin deposited upon biotic and abiotic stresses. Curr. Opin. Biotechnol. 56, 209–214. https://doi.org/10.1016/j.copbio.2018.12.012.
Chaiwanon, J., Wang, Z.-Y., 2015. Spatiotemporal brassinosteroid signaling and antagonism with auxin pattern stem cell dynamics in Arabidopsis roots. Curr. Biol. 25, 1031–1042. https://doi.org/10.1016/j.cub.2015.02.046.
Corpas, F.J., Palma, J.M., Leterrier, M., Río, L.A. del, Barroso, J.B., 2009. Nitric oxide and abiotic stress in higher plants. 51–63. S. Hayat, M. Mori, J. Pichtel, and A. Ahmad (eds) Nitric Oxide in Plant Physiology WILEY-VCH Verlag GmbH & Co.
Correa-Aragunde, N., Foresi, N., Lamattina, L., 2013. Structure diversity of nitric oxide synthases (NOS): the emergence of new forms in photosynthetic organisms. article 232 Front. Plant Sci. 4. https://doi.org/10.3389/fpls.2013.00232.
Della Rovere, F., Fattorini, L., D'Angeli, S., Falasca, G., Altamura, M.M., 2013. Auxin and cytokinin control formation of the quiescent centre in the adventitious root apex of Arabidopsis (https://doi:). Ann. Bot. 112, 1395–1407. https://doi.org/10.1093/aob/mct215.
Della Rovere, F., Piacentini, D., Fattorini, L., Girardi, N., Bellanima, D., Falasca, G., Altamura, M.M., Betti, C., 2022. Brassinosteroids mitigate cadmium effects in Arabidopsis root system without any cooperation with nitric oxide. Int. J. Mol. Sci. 23, 825. https://doi.org/10.3390/ijms23020825.
Devi, L.L., Pandey, A., Gupta, S., Singh, A.P., 2022. The interplay of auxin and brassinosteroid signaling tunes root growth under low and different nitrogen forms. Plant Physiol. 189, 1757–1773. https://doi.org/10.1093/plphys/kiac157.
Dolan, L., Janmaat, K., Willemsen, V., Linstead, P., Poethig, S., Roberts, K., Scheres, B., 1993. Cellular organisation of the *Arabidopsis thaliana* root. Development 119, 71–84. https://doi.org/10.1242/dev.119.1.71.
Emamverdian, A., Ding, Y., Barker, J., Mokhberdoran, F., Ramakrishnan, M., Liu, G., Li, Y., 2021. Nitric oxide ameliorates plant metal toxicity by increasing antioxidant capacity and reducing Pb and Cd translocation. Antioxidants 10, 1981. https://doi.org/10.3390/antiox10121981.
Farooq, S., Singh, S., Kumar, V., Dhanjal, D.S., Ramamurthy, P.C., Singh, J., 2022. Arsenic-induced responses in plants. In: Arsenic in Plants. John Wiley & Sons, Ltd, pp. 99–111. https://doi.org/10.1002/9781119791461.ch5.
Fattorini, L., Ronzan, M., Piacentini, D., Della Rovere, F., De Virgilio, C., Sofo, A., Altamura, M.M., Falasca, G., 2017. Cadmium and arsenic affect quiescent centre formation and maintenance in *Arabidopsis thaliana* post-embryonic roots disrupting auxin biosynthesis and transport. Environ. Exp. Bot. 144, 37–48. https://doi.org/10.1016/j.envexpbot.2017.10.005.
Finnegan, P.M., Chen, W., 2012. Arsenic toxicity: the effects on plant metabolism (https://doi/). Front. Physiol. 3 (182). https://doi.org/10.3389/fphys.2012.00182.
Foresi, N., Correa-Aragunde, N., Parisi, G., Caló, G., Salerno, G., Lamattina, L., 2010. Characterization of a nitric oxide synthase from the plant kingdom: NO generation from the green alga *Ostreococcus tauri* is light irradiance and growth phase dependent. Plant Cell 22, 3816–3830. https://doi.org/10.1105/tpc.109.073510.
Fornara, F., Pařenicová, L., Falasca, G., Pelucchi, N., Masiero, S., Ciannamea, S., Lopez-Dee, Z., Altamura, M.M., Colombo, L., Kater, M.M., 2004. Functional characterization of *OsMADS18*, a member of the *AP1/SQUA* subfamily of MADS box genes. Plant Physiol. 135, 2207–2219. https://doi.org/10.1104/pp.104.045039.
Fridman, Y., Strauss, S., Horev, G., Ackerman-Lavert, M., Reiner-Benaim, A., Lane, B., Smith, R.S., Savaldi-Goldstein, S., 2021. The root meristem is shaped by brassinosteroid control of cell geometry. Nat. Plants 7, 1475–1484. https://doi.org/10.1038/s41477-021-01014-9.
González-García, M.P., Vilarrasa-Blasi, J., Zhiponova, M., Divol, F., Mora-García, S., Russinova, E., Caño-Delgado, A.I., 2011. Brassinosteroids control meristem size by promoting cell cycle progression in Arabidopsis roots. Develop 138, 849–859. https://doi.org/10.1242/dev.057331.
Grün, S., Lindermayer, C., Sell, S., Durner, J., 2006. Nitric oxide and gene regulation in plants. J. Exp. Bot. 57, 507–516. https://doi.org/10.1093/jxb/erj053.
Guedes, F.R.C.M., Maia, C.F., Serrão da Silva, B.R., Batista, B.L., Alyemeni, M.N., Ahmad, P., da Silva Lobato, A.K., 2021. Exogenous 24-epibrassinolide stimulates root protection, and leaf antioxidant enzymes in lead stressed rice plants: central roles to minimize Pb content and oxidative stress (https//doi.org/). Environ. Pollut. 280, 116992. https://doi.org/10.1016/j.envpol.2021.116992.
Guo, F.-Q., Okamoto, M., Crawford, N.M., 2003. Identification of a plant nitric oxide synthase gene involved in hormonal signaling. Science 302, 100–103. https://doi.org/10.1126/science.1086770.
Gupta, K.J., Fernie, A.R., Kaiser, W.M., van Dongen, J.T., 2011. On the origins of nitric oxide. Trends Plant Sci. 16, 160–168. https://doi.org/10.1016/j.tplants.2010.11.007.
Gusman, G.S., Oliveira, J.A., Farnese, F.S., Cambraia, J., 2013. Mineral nutrition and enzymatic adaptation induced by arsenate and arsenite exposure in lettuce plants. Plant Physiol. Biochem. 71, 307–314. https://doi.org/10.1016/j.plaphy.2013.08.00.
Heyman, J., Cools, T., Vandenbussche, F., Heyndrickx, K.S., Van Leene, J., Vercauteren, I., Vanderauwera, S., Vandepoele, K., De Jaeger, G., Van Der Straeten, D., De Veylder, L., 2013. ERF115 controls root quiescent center cell division and stem cell replenishment. Science 342, 860–863. https://doi.org/10.1126/science.1240667.
Horiunova, I.I., Krasylenko, Yu.A., Yemets, A.I., Blume, Ya.B., 2016. Involvement of plant cytoskeleton in cellular mechanisms of metal toxicity. Cytol. Genet. 50, 47–59. https://doi.org/10.3103/S0095452716010060.
Hu, D., Wei, L., Liao, W., 2021. Brassinosteroids in plants: crosstalk with small-molecule compounds. Biomolecules 11, 1800. https://doi.org/10.3390/biom11121800.
Hurali, D.T., Bhurta, R., Tyagi, S., Sathee, L., Sandeep, A.B., Singh, D., Mallick, N., Vinod, Jha, S.K., 2022. Analysis of *NIA* and *GSNOR* family genes and nitric oxide homeostasis in response to wheat-leaf rust interaction. Sci. Rep. 12, 803. https://doi.org/10.1038/s41598-021-04696-5.
Jan, S., Alyemeni, M.N., Wijaya, L., Alam, P., Siddique, K.H., Ahmad, P., 2018. Interactive effect of 24-epibrassinolide and silicon alleviates cadmium stress via the modulation of antioxidant defense and glyoxalase systems and macronutrient content in *Pisum sativum* L. seedlings. BMC Plant Biol. 18, 146. https://doi.org/10.1186/s12870-018-1359-5.
Jantapo, K., Wimonchaijt, W., Wang, W., Chaiwanon, J., 2021. Supraoptimal brassinosteroids levels inhibit root growth by reducing root meristem and cell elongation in rice. Plants 10, 1962. https://doi.org/10.3390/plants10091962.
Kanvar, M.K., Poonam, Bhardwaj, R., 2015. Arsenic induced modulation of antioxidative defense system and brassinosteroids in *Brassica juncea* L. Ecotoxcol. Environ. Saf. 115, 119–125. https://doi.org/10.1016/j.ecoenv.2015.02.016.
Kaya, C., Ashraf, M., Alyemeni, M.N., Corpas, F.J., Ahmad, P., 2020. Salicylic acid-induced nitric oxide enhances arsenic toxicity tolerance in maize plants by upregulating the ascorbate-glutathione cycle and glyoxalase system. J. Hazard. Mater. 399, 123020 https://doi.org/10.1016/j.jhazmat.2020.123020.
Kidwai, M., Dhar, Y.V., Gautam, N., Tiwari, M., Ahmad, I.Z., Asif, M.H., Chakrabarty, D., 2018. *Oryza sativa* class III peroxidase (*OsPRX38*) overexpression in *Arabidopsis thaliana* reduces arsenic accumulation due to apoplastic lignification. J. Hazard. Mater. 362, 383–393. https://doi.org/10.1016/j.jhazmat.2018.09.029.
Kushwaha, B.K., Singh, S., Tripathi, D.K., Sharma, S., Prasad, S.M., Chauhan, D.K., Kumar, V., Singh, V.P., 2019. New adventitious root formation and primary root biomass accumulation are regulated by nitric oxide and reactive oxygen species in rice seedlings under arsenate stress. J. Hazard. Mater. 361, 134–140. https://doi.org/10.1016/j.jhazmat.2018.08.035.
Lanza, M., Garcia-Ponce, B., Castrillo, G., Catarecha, P., Sauer, M., Rodriguez-Serrano, M., Páez-García, A., Sánchez-Bermejo, E., Tc, M., Leo del Puerto, Y., Sandalio, L.M., Paz-Ares, J., Leyva, A., 2012. Role of actin cytoskeleton in brassinosteroid signaling and in its integration with the auxin response in plants. Dev. Cell 22, 1275–1285. https://doi.org/10.1016/j.devcel.2012.04.008.
Li, Y., Wu, Y., Liao, W., Hu, L., Dawuda, M.M., Jin, X., Tang, Z., Yang, J., Yu, J., 2020. Nitric oxide is involved in the brassinolide-induced adventitious root development in cucumber. BMC Plant Biol. 20, 102. https://doi.org/10.1186/s12870-020-2320-y.
Liscum, E., Reed, J.W., 2002. Genetics of Aux/IAA and ARF action in plant growth and development. Plant Mol. Biol. 49, 387–400. https://doi.org/10.1023/A:1015255030047.
Lou, L.Q., Shi, G.L., Wu, J.H., Zhu, S., Qian, M., Wang, H.Z., Cai, Q.S., 2015. The influence of phosphorus on arsenic uptake/efflux and As toxicity to wheat roots in comparison with sulfur and silicon. J. Plant Growth Regul. 34, 242–250. https://doi.org/10.1007/s00344-014-9460-y.
Ma, J.F., Yamaji, N., Mitani, N., Xu, X.-Y., Su, Y.-H., McGrath, S.P., Zhao, F.-J., 2008. Transporters of arsenite in rice and their role in arsenic accumulation in rice grain. Proc. Natl. Acad. Sci. U.S.A. 105, 9931–9935. https://doi.org/10.1073/pnas.0802361105.
Mansoor, S., Wani, O.A., Lone, J.K., Manhas, S., Kour, N., Alam, P., Ahmad, A., Ahmad, P., 2022. Reactive oxygenspecies in plants: from source to sink. Antioxidants 11, 225. https://doi.org/10.3390/antiox11020225.
Mendoza-Cózatl, D.G., Jobe, T.O., Hauser, F., Schroeder, J.I., 2011. Long distance transport, vacuolar sequestration, tolerance, and transcriptional responses induced by cadmium and arsenic (https//doi/). Curr. Opin. Plant Biol. 14, 554–562. https://doi.org/10.1016/j.pbi.2011.07.004.
Meng, Y., Jing, H., Huang, J., Shen, R., Zhu, X., 2022. The role of nitric oxide signaling in plant responses to cadmium stress. Int. J. Mol. Sci. 23, 6901. https://doi.org/10.3390/ijms23136901.
Mondal, N.K., Debnath, P., Mishra, D., 2022. Impact of inorganic arsenic (III and V) on growth and development of rice (*Oryza sativa* L.) with special emphasis on root and coleoptile growth. Environ. Process. 9, 31. https://doi.org/10.1007/s40710-022-00586-8.
Moura, J.C.M.S., Bonine, C.A.V., De Oliveira Fernandes Viana, J., Dornelas, M.C., Mazzafera, P., 2010. Abiotic and biotic stresses and changes in the lignin content and composition in plants. J. Integr. Plant Biol. 52, 360–376. https://doi.org/10.1111/j.1744-7909.2010.00892.x.
Murashige, T., Skoog, F., 1962. A revised medium for rapid growth and bioassays with tobacco tissue cultures. Physiol. Plant. 15, 473–497. https://doi.org/10.1111/j.1399-3054.1962.tb08052.x.
Ni, J., Shen, Y., Zhang, Y., Wu, P., 2014. Definition and stabilisation of the quiescent centre in rice roots. Plant Biol. 16, 1014–1019 https://doi.org/10.1111/plb. 12138.
Nolan, T.M., Vukašinović, N., Liu, D., Russinova, E., Yin, Y., 2020. Brassinosteroids: multidimensional regulators of plant growth, development, and stress responses. Plant Cell 32, 295–318. https://doi.org/10.1105/tpc.19.00335.
Pardal, R., Heidstra, R., 2021. Root stem cell niche networks: it's complexed! Insights from Arabidopsis. J. Exp. Bot. 13, 6727–6738. https://doi.org/10.1093/jxb/erab272.
Parrotta, L., Guerriero, G., Sergeant, K., Cai, G., Hausman, J.F., 2015. Target or barrier? The cell wall of early-and lateral-diverging plants vs cadmium toxicity: differences in the response mechanisms. Front. Plant Sci. 6, 133 https://doi.org/110.3389/fpls.2015.00133.
Piacentini, D., Ronzan, M., Fattorini, L., Della Rovere, F., Massimi, L., Altamura, M.M., Falasca, G., 2020a. Nitric oxide alleviates cadmium- but not arsenic-induced damages in rice roots. Plant Physiol. Biochem. 151, 729–742. https://doi.org/10.1016/j.plaphy.2020.04.004.
Piacentini, D., Corpas, F.J., D'Angeli, S., Altamura, M.M., Falasca, G., 2020b. Cadmium and arsenic-induced-stress differentially modulates Arabidopsis root architecture, peroxisome distribution, enzymatic activities and their nitric oxide content. Plant Physiol. Biochem. 148, 312–323. https://doi.org/10.1016/j.plaphy.2020.01.026.
Praveen, A., Gupta, M., 2018. Nitric oxide confronts arsenic stimulated oxidative stress and root architecture through distinct gene expression of auxin transporters, nutrient

related genes and modulates biochemical responses in Oryza sativa L. Environ. Pollut. 240, 950–962. https://doi.org/10.1016/j.envpol.2018.04.096.
Raghu, K., Mahesh, K., Divya Sri, N., Rao, S.S.R., 2014. Effect of brassinosteroids on the seed germination and seedling growth of radish (*Raphanus sativus* L) under arsenic toxicity stress. Int. J. Dev. Res. 9, 1929–1933.
Rajewska, I., Talarek, M., Bajguz, A., 2016. Brassinosteroids and response of plants to heavy metal action. Front. Plant Sci. 7, 629. https://doi.org/10.3389/fpls.2016.00629.
Rao, X., Dixon, R.A., 2017. Brassinosteroid mediated cell wall remodeling in grasses under abiotic stress. Front. Plant Sci. 8, 806. https://doi.org/10.3389/fpls.2017.00806.
Ronzan, M., Piacentini, D., Fattorini, L., Della Rovere, F., Eiche, E., Riemann, M., Altamura, M.M., Falasca, G., 2018. Cadmium and arsenic affect root development in *Oryza sativa* L. negatively interacting with auxin. Environ. Exp. Bot. 151, 64–75. https://doi.org/10.1016/j.envexpbot.2018.04.008.
Sahni, S., Prasad, B.D., Liu, Q., Grbic, V., Sharpe, A., Singh, S.P., Krishna, P., 2016. Overexpression of the brassinosteroid biosynthetic gene *DWF4* in *Brassica napus* simultaneously increases seed yield and stress tolerance. Sci. Rep. 6, 28298. https://doi.org/10.1038/srep28298.
Samal, A.C., Bhattacharya, P., Biswas, P., Maity, J.P., Bundschuh, J., Santra, S.C., 2021. Variety-specific arsenic accumulation in 44 different rice cultivars (*O. sativa* L.) and human health risks due to co-exposure of arsenic-contaminated rice and drinking water. J. Hazard. Mater. 407, 124804 https://doi.org/10.1016/j.jhazmat.2020.124804.
Simontacchi, M., Galatro, A., Ramos-Artuso, F., Santa-María, G.E., 2015. Plant survival in a changing environment: the role of nitric oxide in plant responses to abiotic stress. Front. Plant Sci. 6, 977. https://doi.org/10.3389/fpls.2015.00977.
Song, W.Y., Mendoza-Cózatl, D.G., Lee, Y., Schroeder, J.I., Ahn, S.N., Lee, H.S., Wicker, T., Martinoia, E., 2014. Phytochelatin- metal(loid) transport into vacuoles shows different substrate preferences in barley and Arabidopsis (htpps://doi/). Plant Cell Environ. 37, 1192–1201. https://doi.org/10.1111/pce.12227.
Stuehr, D.J., 1999. Mammalian nitric oxide synthases. Biochim. Biophys. Acta BBA - Bioenergy 1411, 217–230. https://doi.org/10.1016/S0005-2728(99)00016-X.
Tossi, V., Lamattina, L., Cassia, R., 2013. Pharmacological and genetical evidence supporting nitric oxide requirement for 2,4-epibrassinolide regulation of root architecture in *Arabidopsis thaliana*. e24712 Plant Signal. Behav. 8. https://doi.org/10.4161/psb.24712.
Vaddepalli, P., de Zeeuw, T., Strauss, S., Bürstenbinder, K., Liao, C.Y., Ramlho, J.J., Smith, R.S., Weijers, D., 2021. Auxin-dependent control of cytoskeleton and cell shape regulate division orientation in the Arabidopsis embryo. e4 Curr. Biol. 31, 4946–4955. https://doi.org/10.1016/j.cub.2021.09.019.
Vardhini, B.V., 2017. Modifications of morphological and anatomical characteristics of plants by application of brassinosteroids under various abiotic stress conditions - a review. Plant Gene 11, 70–89. https://doi.org/10.1016/j.plgene.2017.06.005.
Vardhini, B.V., Anjum, N.A., 2015. Brassinosteroids make plant life easier under abiotic stresses mainly by modulating major components of antioxidant defense system. Front. Environ. Sci. 2, 2014. https://doi.org/10.3389/fenvs.2014.00067.
Vilarrasa-Blasi, J., González-García, M.P., Frigola, D., Fàbregas, N., Alexiou, K.G., López-Bigas, N., Rivas, S., Jauneau, A., Lohmann, J.U., Benfey, P.N., Ibañes, M., Caño-Delgado, A.I., 2014. Regulation of plant stem cell quiescence by a brassinosteroids signal module. Dev. Cell 14, 36–47. https://doi.org/10.1016/j.devcel.2014.05.020.
Wang, M., Yang, K., Le, J., 2015. Organ-specific effects of brassinosteroids on stomatal production coordinate with the action of *TOO MANY MOUTHS*. J. Integr. Plant Biol. 57, 247–255. https://doi.org/10.1111/jipb.12285.
Weigel, D., Glazebrook, J., 2002. Arabidopsis: A Laboratory Manual. CSHL Press.
Wu, X.X., Chen, J.L., Xu, S., Zhu, Z.W., Zha, D.S., 2016. Exogenous 24-epibrassinolide alleviates zinc-induced toxicity in eggplant (*Solanum melongena* L.) seedlings by regulating the glutathione-ascorbate-dependent detoxification pathway. J. Hortic. Sci. Biotechnol. 91, 412–420. https://doi.org/10.1080/14620316.2016.1162030.
Yang, C.-J., Zhang, C., Lu, Y.-N., Jin, J.-Q., Wang, X.-L., 2011. The mechanisms of brassinosteroids' action: from signal transduction to plant development. Mol. Plant 4, 588–600. https://doi.org/10.1093/mp/ssr020.
Yang, J., Yuan, Z., Meng, Q., Huang, G., Périn, C., Bureau, C., Meunier, A.C., Ingouff, M., Bennet, M.J., Liang, W., Zhang, D., 2017. Dynamic regulation of auxin response during rice development revealed by newly established hormone biosensor markers (https//doi/). Front. Plant Sci. 8, 256. https://doi.org/10.3389/fpls.2017.00256.
Ye, Y., Godzik, A., 2004. FATCAT: a web server for flexible structure comparison and structure similarity searching. W582–W585 Nucleic Acids Res. 32. https://doi.org/10.1093/nar/gkh430.
Zhang, H., Zhao, D., Tang, Z., Zhang, Y., Zhang, K., Dong, J., Wang, F., 2022. Exogenous brassinosteroids promotes root growth, enhances stress tolerance, and increases yield in maize. Plant Signal. Behav. 17, 2095139 https://doi.org/10.1080/15592324.2022.2095139.
Zluhan-Martínez, E., López-Ruíz, B.A., García-Gómez, M.L., García-Ponce, B., de la Paz Sánchez, M., Álvarez-Buylla, E.R., Garay-Arroyo, A., 2021. Integrative roles of phytohormones on cell proliferation, elongation and differentiation in the *Arabidopsis thaliana* primary root. Front. Plant Sci. 12. https://doi.org/10.3389/fpls.2021.659155.
Zvobgo, G., 2022. Arsenic transport and metabolism in plants. In: Arsenic in Plants. John Wiley & Sons, Ltd, pp. 49–63. https://doi.org/10.1002/9781119791461.ch3.